9-2-2008

Observational Tests of Modified Gravity

Bhuvnesh Jain
University of Pennsylvania, bjain@physics.upenn.edu

Pengjie Zhang
Shanghai Astronomical Observatory; Joint Institute for Galaxy and Cosmology

http://dx.doi.org/10.1103/PhysRevD.78.063503

Observational Tests of Modified Gravity

Abstract
Modifications of general relativity provide an alternative explanation to dark energy for the observed acceleration of the Universe. Modified gravity theories have richer observational consequences for large scale structures than conventional dark energy models, in that different observables are not described by a single growth factor even in the linear regime. We examine the relationships between perturbations in the metric potentials, density and velocity fields, and discuss strategies for measuring them using gravitational lensing, galaxy cluster abundances, galaxy clustering/dynamics, and the integrated Sachs-Wolfe effect. We show how a broad class of gravity theories can be tested by combining these probes. A robust way to interpret observations is by constraining two key functions: the ratio of the two metric potentials, and the ratio of the gravitational "constant" in the Poisson equation to Newton's constant. We also discuss quasilinear effects that carry signatures of gravity, such as through induced three-point correlations. Clustering of dark energy can mimic features of modified gravity theories and thus confuse the search for distinct signatures of such theories. It can produce pressure perturbations and anisotropic stresses, which break the equality between the two metric potentials even in general relativity. With these two extra degrees of freedom, can a clustered dark energy model mimic modified gravity models in all observational tests? We show with specific examples that observational constraints on both the metric potentials and density perturbations can in principle distinguish modifications of gravity from dark energy models. We compare our result with other recent studies that have slightly different assumptions (and apparently contradictory conclusions).

Disciplines
Physical Sciences and Mathematics | Physics

Comments
Suggested Citation:
B. Jain and P. Zhang. (2008). "Observational tests of modified gravity." *Physical Review D.* **78**, 063503.

http://dx.doi.org/10.1103/PhysRevD.78.063503

PHYSICAL REVIEW D **78,** 063503 (2008)

Observational tests of modified gravity

Bhuvnesh Jain[1] and Pengjie Zhang[2,3,*]

[1]*Department of Physics and Astronomy, University of Pennsylvania, Philadelphia, Pennsylvania 19104, USA*
[2]*Shanghai Astronomical Observatory, Shanghai, China 200030*
[3]*Joint Institute for Galaxy and Cosmology (JOINGC) of Shanghai Astronomical Observatory (SHAO) and University of Science and Technology of China (USTC), 80 Nandan Road, Shanghai, China 200030*

(Received 8 October 2007; published 2 September 2008)

Modifications of general relativity provide an alternative explanation to dark energy for the observed acceleration of the Universe. Modified gravity theories have richer observational consequences for large-scale structures than conventional dark energy models, in that different observables are not described by a single growth factor even in the linear regime. We examine the relationships between perturbations in the metric potentials, density and velocity fields, and discuss strategies for measuring them using gravitational lensing, galaxy cluster abundances, galaxy clustering/dynamics, and the integrated Sachs-Wolfe effect. We show how a broad class of gravity theories can be tested by combining these probes. A robust way to interpret observations is by constraining two key functions: the ratio of the two metric potentials, and the ratio of the gravitational ''constant'' in the Poisson equation to Newton's constant. We also discuss quasilinear effects that carry signatures of gravity, such as through induced three-point correlations. Clustering of dark energy can mimic features of modified gravity theories and thus confuse the search for distinct signatures of such theories. It can produce pressure perturbations and anisotropic stresses, which break the equality between the two metric potentials even in general relativity. With these two extra degrees of freedom, can a clustered dark energy model mimic modified gravity models in all observational tests? We show with specific examples that observational constraints on both the metric potentials and density perturbations can in principle distinguish modifications of gravity from dark energy models. We compare our result with other recent studies that have slightly different assumptions (and apparently contradictory conclusions).

DOI: 10.1103/PhysRevD.78.063503 PACS numbers: 98.65.Dx, 04.50.Kd, 95.36.+x

I. INTRODUCTION

The energy contents of the Universe pose an interesting puzzle, in that general relativity (GR) plus the standard model of particle physics can only account for about 4% of the energy density inferred from observations. By introducing dark matter (DM) and dark energy (DE), which account for the remaining 96% of the total energy budget of the Universe, cosmologists have been able to account for a wide range of observations, from the overall expansion of the Universe to the large-scale structure of the early and late Universe [1].

The dark matter/dark energy scenario assumes the validity of GR at galactic and cosmological scales and introduces exotic components of matter and energy to account for observations. Since GR has not been tested independently on these scales, a natural alternative is that the failures of GR plus the standard model of particle physics imply a failure of GR. This possibility, that modifications in GR at galactic and cosmological scales can replace dark matter and/or dark energy, has become an area of active research in recent years.

Attempts have been made to modify GR at galactic [2] or cosmological scales [3–5]. Modified Newtonian dynamics and its relativistic version (tensor-vector-scalar, TeVeS) [2] are able to replace dark matter at galaxy scales to reproduce the galaxy rotation curves, which provided the earliest and most direct evidences for the existence of dark matter. The DGP model [3], in which gravity lives in a 5D brane world, naturally leads to late time acceleration of the Universe. Adding a correction term $f(R)$ to the Einstein-Hilbert action [4] also allows late time acceleration of the Universe to be realized.

In this paper we will focus on modified gravity (MG) theories that are designed as an alternative to dark energy to produce the present day acceleration of the Universe. In these models, such as DGP and $f(R)$ models, gravity at late cosmic times and on large scales departs from the predictions of GR. We will consider the prospects of distinguishing MG models containing dark matter but no dark energy from GR models with dark matter and dark energy. By design, successful MG models will be indistinguishable from viable DE models against observations of the expansion history of the Universe. To break this degeneracy, observations of large-scale structure (LSS) must be used to test the growth of perturbations.

LSS in MG theories can be more complicated to predict, but is also richer because different observables such as lensing and galaxy clustering probe independent perturbed variables. This differs from conventional DE scenarios

*bjain@physics.upenn.edu

where the linear growth factor of the density field fixes all observables on sufficiently large scales. One of the goals of this study is to examine carefully what various LSS observables measure once the assumption of GR (with smooth DE) is dropped.

Structure formation in modified gravity in general differs [6–18] from that in GR. Theories of LSS in these modified gravity models are still in their infancy. However, perturbative calculations at large scales have shown that it is promising to connect predictions in these theories with observations of LSS. Most studies have focused on probes of a single growth factor with one or a few observables. In this paper we will consider a variety of LSS observables that can be measured with high precision with current or planned surveys. Our emphasis will be on model-independent constraints of MG enabled by combining different observables.

Carrying out robust tests of MG in practice is challenging as in the absence of a fundamental theory, the modifications to gravity are often parametrized by free functions, to be fine-tuned and fixed by observations. Given the parameter space available to both DE and MG theories, it is unclear how the two classes of theories can be distinguished. Kunz and Sapone [19] presented a rather pessimistic example. They found that one can tune a clustered dark energy model to reproduce observations of gravitational lensing and matter fluctuations in the DGP model. It is not clear if this conclusion applies to all modified gravity models and if adding more LSS observables helps to break this severe degeneracy.

In this paper, we first discuss ways of parametrizing modified gravity models and dark energy models. Section II presents the definitions and evolution equations for perturbations in the metric and the energy-momentum tensor. We then classify independent LSS observables based on the perturbations that are probed by them. Section III is devoted to the use of observational probes of LSS for testing MG. We consider the four fundamental perturbation variables and the observations that can be used to probe them. The additional information available in the quasilinear regime is discussed in the Appendix. In Sec. IV we consider the question of distinguishing MG from DE scenarios. The specific question we want to answer is: given a set of LSS observations, can a general MG model be mimicked by a DE model? If not, what LSS observables are required to break the degeneracy? We conclude in Sec. V.

II. PERTURBATION FORMALISM

By definition, the dark sector (dark matter and dark energy) can only be inferred from their gravitational consequence. In general relativity, gravity is determined by the total stress-energy tensor of all matter and energy ($G_{\mu\nu} = 8\pi G T_{\mu\nu}$). Thus we can treat dark matter and dark energy as a single entity, without loss of physical generality [20–22]. This entity has total mean matter density $\bar{\rho}_{\rm GR}$ and equation of state parameter $w = p_{\rm GR}/\bar{\rho}_{\rm GR}$. However, when discussing perturbations in this entity, we may separate it into a matter component (dissipationless particles which can be described as a pressureless fluid free of anisotropic stress) and a dark energy component. Throughout this paper, when we refer to ''smooth'' or ''clustered'' dark energy, we refer to this dark energy subset of the overall dark sector.

We may consider the Hubble parameter $H(z)$ to be fixed by observations. In a dark energy model, $\bar{\rho}_{\rm GR}$ is given by the Friedmann equation of GR: $\bar{\rho}_{\rm GR} = 3H^2/8\pi G$. The equation of state parameter is $w = -1 - 2\dot{H}/3H^2$.

The corresponding modified gravity model has matter density $\bar{\rho}_{\rm MG}$ to be determined from its Friedmann-like equation. We will consider MG models dominated by dark matter and baryons at late times and denote fluid variables such as the density with subscript MG.

A. Metric and fluid perturbations

With the smooth variables fixed, we will consider perturbations as a way of testing the models. In the Newtonian gauge, scalar perturbations to the metric are fully specified by two scalar potentials ψ and ϕ:

$$ds^2 = -(1 + 2\psi)dt^2 + (1 - 2\phi)a^2(t)d\vec{x}^2, \qquad (1)$$

where $a(t)$ is the expansion scale factor. This form for the perturbed metric is fully general for any metric theory of gravity, aside from having excluded vector and tensor perturbations (see [23] and references therein for justifications). Note that ψ corresponds to the Newtonian potential for the acceleration of particles, and that in general relativity $\phi = \psi$ in the absence of anisotropic stresses.

A metric theory of gravity relates the two potentials above to the perturbed energy-momentum tensor. We introduce variables to characterize the density and velocity perturbations for a fluid, which we will use to describe matter and dark energy (we will also consider pressure and anisotropic stress below). The density fluctuation δ is given by

$$\delta(\vec{x}, t) \equiv \frac{\rho(\vec{x}, t) - \bar{\rho}(t)}{\bar{\rho}(t)}, \qquad (2)$$

where $\rho(\vec{x}, t)$ is the density and $\bar{\rho}(t)$ is the cosmic mean density. The second fluid variable is the divergence of the peculiar velocity

$$\theta \equiv \nabla_j T^j_0/(\bar{p} + \bar{\rho}) = \vec{\nabla} \cdot \vec{v}, \qquad (3)$$

where $\vec{v}$ is the (proper) peculiar velocity. Choosing θ instead of the vector $\mathbf{v}$ implies that we have assumed $\mathbf{v}$ to be irrotational. This approximation is sufficiently accurate in the linear regime, even for unconventional dark energy models and minimally coupled modified gravity models.

In principle, observations of large-scale structure can directly measure the four perturbed variables introduced

above: the two scalar potentials ψ and ϕ, and the density and velocity perturbations specified by δ and θ. As shown below, these variables are the key to distinguishing modified gravity models from dark energy. Each has a scale and redshift dependence, so it is worth noting which variables and at what scale and redshift are probed by different observations. It is convenient to work with the Fourier transforms, such as

$$\hat{\delta}(\vec{k}, t) = \int d^3x \delta(\vec{x}, t) e^{-i\vec{k}\cdot\vec{x}}. \tag{4}$$

When we refer to length scale λ, it corresponds to a statistic such as the power spectrum on wave number $k = 2\pi/\lambda$. We will henceforth work exclusively with the Fourier space quantities and drop the $\hat{}$ symbol for convenience.

B. Evolution and constraint equations

We consider here the fluid equations for DE and MG scenarios. We work in the Newtonian gauge and follow the formalism and notation of [20], except that we use physical time t instead of conformal time. We are interested in the evolution of perturbations after decoupling, so we will neglect radiation and neutrinos as sources of perturbations. We will make the approximation of nonrelativistic motions and restrict ourselves to subhorizon length scales. One can also self-consistently neglect time derivatives of the metric potentials in comparison to spatial gradients. These approximations will be referred to as the quasistatic, Newtonian regime. We will not consider the evolution of perturbations on superhorizon length scales; [24] shows that differences in their evolution may have observable consequences for some MG models [discussed further under the cosmic microwave background (CMB) below].

1. Dark energy with GR scenario

We first consider the DE scenario, assuming GR. Using the perturbed field equations of GR to first order gives a set of constraint and evolution equations. The evolution of the density and velocity perturbations includes gravity and pressure perturbations δp as sources. In the Newtonian limit they give the familiar continuity and Euler equations for a perfect fluid. Keeping all first order terms and using the notation $\dot{\delta} \equiv d\delta/dt$, gives

$$\begin{aligned}\dot{\delta}_{\rm GR} &= -(1+w)\left(\frac{\theta_{\rm GR}}{a} - 3\dot{\phi}\right) - 3H\frac{\delta p}{\rho} + 3Hw\delta_{\rm GR} \\ &\simeq -(1+w)\frac{\theta_{\rm GR}}{a} - 3H\frac{\delta p}{\rho} + 3Hw\delta_{\rm GR}.\end{aligned} \tag{5}$$

In the second line we have dropped the $\dot{\phi}$ term as it is negligible compared to the other terms in the quasistatic regime. The Euler equation is given by

$$\begin{aligned}\dot{\theta}_{\rm GR} &= -H(1-3w)\theta_{\rm GR} - \frac{\dot{w}}{1+w}\theta_{\rm GR} \\ &\quad + \left(\frac{\delta p/\rho}{1+w} - \sigma + \psi\right)\frac{k^2}{a}.\end{aligned} \tag{6}$$

We have allowed for anisotropic stress sources in the energy-momentum tensor, parametrized by the scalar σ, which enters the Euler equation.

Note that the above equations describe the multicomponent fluid of baryons, dark matter, and dark energy; the density and velocity variables for this fluid are subscripted GR above (these variables will represent a fluid with no dark energy for MG theories below). The metric potential variables are ϕ and ψ in either case. Further, we do not subscript δp and σ as these sources occur only in the DE plus GR scenario.

The linearized constraint equation gives the Poisson equation for weak field gravity:

$$\begin{aligned}k^2\phi &= -4\pi G a^2 \bar{\rho}_{\rm GR}\left[\delta_{\rm GR} + 3(1+w)Ha\frac{\theta_{\rm GR}}{k^2}\right], \\ &\simeq -4\pi G a^2 \bar{\rho}_{\rm GR}\delta_{\rm GR},\end{aligned} \tag{7}$$

where in the second line we have dropped the $H\theta_{\rm GR}/k^2$ term as it is negligible for nonrelativistic motions on scales well below the horizon.

Nonzero anisotropic stress σ leads to inequality between the two potentials:

$$k^2(\phi - \psi) = 12\pi G a^2(1+w)\bar{\rho}\sigma. \tag{8}$$

It is common to take $\phi = \psi$ for ordinary matter and dark matter; however clustered dark energy can have a non-negligible anisotropic stress.

Equations (5)–(8) fully describe the evolution of perturbations in DE scenarios in the quasistatic, Newtonian regime. Next we consider the analogous relations for modified gravity scenarios.

2. Modified gravity scenario

For minimally coupled gravity models with baryons and cold dark matter, but without dark energy, we can neglect pressure and anisotropic stress terms in the evolution equations to get the continuity equation:

$$\dot{\delta}_{\rm MG} = -\left(\frac{\theta_{\rm MG}}{a} - 3\dot{\phi}\right) \simeq -\frac{\theta_{\rm MG}}{a}, \tag{9}$$

where the second equality follows from the quasistatic approximation as for GR. The Euler equation is

$$\dot{\theta}_{\rm MG} = -H\theta_{\rm MG} + \frac{k^2\psi}{a}. \tag{10}$$

For a generic MG theory, the analog of the constraint equations (7) and (8) can take different forms. We will attempt to characterize the general behavior in the weak field limit for small perturbations (small δ) and nonrela-

tivistic motions. On subhorizon scales the field equations in MG theories can then be significantly simplified. We parametrize modifications in gravity by two functions $\tilde{G}_{\rm eff}(k,t)$ and $\eta(k,t)$ to get the analog of the Poisson equation and a second equation connecting ϕ and ψ [25]. We first write the generalization of the Poisson equation in terms of an effective gravitational constant $G_{\rm eff}$:

$$k^2\phi = -4\pi G_{\rm eff}(k,t)\bar{\rho}_{\rm MG}a^2\delta_{\rm MG}. \tag{11}$$

Note that the potential ϕ in the Poisson equation comes from the spatial part of the metric, whereas it is the "Newtonian" potential ψ that appears in the Euler equation (it is called the Newtonian potential as its gradient gives the acceleration of material particles). Thus in MG, one cannot directly use the Poisson equation to eliminate the potential in the Euler equation. A more useful version of the Poisson equation would relate the sum of the potentials, which determines lensing, with the mass density. We therefore introduce $\tilde{G}_{\rm eff}$ and write the constraint equations for MG as

$$k^2(\psi+\phi) = -8\pi\tilde{G}_{\rm eff}(k,t)\bar{\rho}_{\rm MG}a^2\delta_{\rm MG}, \tag{12}$$

$$\phi = \psi\eta(k,t), \tag{13}$$

where $\tilde{G}_{\rm eff} = G_{\rm eff}(1+\eta^{-1})/2$. Note that if one starts in real space then the corresponding parameters would not be Fourier transforms of η and $\tilde{G}_{\rm eff}$. Thus the Fourier transform of the parametrized post-Newtonian parameter $\gamma \equiv \phi/\psi$, the ratio of the metric potentials in real space constrained by solar system tests, is given by a convolution of η and ψ [26]. Only if η is scale independent would it be the Fourier transform of γ. A similar reasoning applies to $\tilde{G}_{\rm eff}$ in using the Poisson equation. We prefer to work in Fourier space because of the ease of describing perturbations: each Fourier mode evolves independently in the large-scale, linear regime. Furthermore, the equations describing cosmological perturbations in MG theories such as $f(R)$ gravity and DGP are generally expressed in Fourier space.

The parameter $\tilde{G}_{\rm eff}$ characterizes deviations in the $(\psi+\phi)-\delta$ relation from that in GR. Since the combination $\psi+\phi$ is directly responsible for gravitational lensing, $\tilde{G}_{\rm eff}$ has a specific physical meaning: it determines the power of matter inhomogeneities to distort light. This is the reason we prefer it over working with more direct generalization of Newton's constant, $G_{\rm eff}$.

The $\tilde{G}_{\rm eff}-\eta$ parametrization is equivalent to the $Q-\eta$ parametrization independently proposed by [18] (see also [27]), where Q parametrizes deviations in Poisson equation (7) from GR. For minimally coupled gravity models, with no dark energy fluctuations, it is also equivalent to that proposed by [16]. And η is also equivalent to the parameter ϖ proposed by [17]. DGP and $f(R)$ gravity can be described by our parametrization. So is the widely adopted Yukawa potential. An exception to our approach is TeVeS as it includes scalar and vector fields that are coupled to the growth of scalar perturbations.

For a generic metric theory of MG, one would expect that a Poisson-like equation is valid to leading order in the potentials and the density perturbation, at least on large scales in the linear regime where Fourier modes are uncoupled. In this regime, we expect that since the left-hand side of the field equations involves curvature, it must have second derivatives of the metric perturbations, while the right-hand side is simply given by the energy-momentum tensor. On smaller scales, in general a MG theory may not obey superposition and require higher order terms and higher derivatives of the potentials. Similarly a generic relation between ϕ and ψ is likely to have a linearized relation of the form in Eq. (13). While it is not necessary that the leading term be linear in both the potentials, observational constraints require that it be very close to linear with $\eta \simeq 1$ on small scales where tests of gravity exist (see [28] for a review).

With the linearized equations above, the evolution of either the density or velocity perturbations can be described by a single second order differential equation. In the case of MG theories, this equation is simpler as the only source is provided by the Newtonian potential ψ. From Eqs. (9) and (10) we get, for the linear solution, $\delta(\vec{k},t) \simeq \delta_{\rm initial}(\vec{k})D(k,t)$,

$$\ddot{\delta} + 2H\dot{\delta} + \frac{k^2\psi}{a} = 0. \tag{14}$$

For a given theory, Eqs. (12) and (13) then allow us to substitute for ψ in terms of δ to determine $D(k,t)$, the linear growth factor for the density:

$$\ddot{D} + 2H\dot{D} - \frac{8\pi\tilde{G}_{\rm eff}}{(1+\eta)}\bar{\rho}_{\rm MG}a^2D = 0. \tag{15}$$

We can also use the relations given above to obtain the linear growth factors for θ and the potentials from D. Note that in general the growth factors for the potentials have a different k dependence than D. In the Appendix we give details on the linear and second order solutions and summarize quasilinear signatures of MG theories.

C. Power spectra

Before we turn to large-scale structure observables, we define the power spectra of the perturbed variables. The three-dimensional power spectrum of $\delta(k,z)$ for instance is defined as

$$\langle\delta(\vec{k},z)\delta(\vec{k}',z)\rangle = (2\pi)^3\delta_{\rm D}(\vec{k}+k')P_\delta(k,z), \tag{16}$$

where we have switched the time variable to redshift z. The power spectra of perturbations in other quantities are defined analogously. We will denote the cross spectra of two different variables with appropriate subscripts, for ex-

ample, $P_{\delta\psi}$ denotes the cross spectrum of the density δ and the potential ψ.

We write down next the relation between the power spectra of the two potentials and the density in DE and MG scenarios. From the Poisson equation (7) for GR we have

$$\text{GR}: P_\phi(k,z) = (4\pi G)^2 a^4 \bar{\rho}_{\rm GR}^2 \frac{P_{\delta,\rm GR}(k,z)}{k^4}, \tag{17}$$

where P_ϕ is the power spectrum of the potential ϕ. Using the Friedmann equation for GR the above equation is often written as

$$\text{GR}: P_\phi(k,z) = \frac{9}{4} H_0^2 \Omega^2 \frac{P_{\delta,\rm GR}(k,z)}{a^2 k^4}, \tag{18}$$

where H_0 is the present day value of the Hubble parameter, and Ω is the dimensionless density parameter.

The Poisson equation (12) for MG gives the following equations for the power spectra of the metric potentials:

$$\begin{aligned}\text{MG: } P_{\psi+\phi}(k,z) &= [8\pi\tilde{G}_{\rm eff}(k,z)]^2 a^4 \bar{\rho}_{\rm MG}^2 P_{\delta,\rm MG}(k,z)/k^4 \\ \text{or} \quad P_\phi &= \frac{[8\pi\tilde{G}_{\rm eff}(k,z)]^2}{[1+\eta^{-1}(k,z)]^2} a^4 \bar{\rho}_{\rm MG}^2 \frac{P_{\delta,\rm MG}(k,z)}{k^4},\end{aligned} \tag{19}$$

where we have used Eq. (13) to get the equation for P_ϕ.

For LSS observables, we will need the power spectra of $(\psi+\phi)$ for lensing, of ψ for dynamics, and of δ for tracers of LSS. We will use Eqs. (17)–(19) to connect them, along with the relations between the two potentials [Eq. (8) for GR and Eq. (13) for MG]. With these relations we can express different observable power spectra in terms of a single density power spectrum—for MG this will involve the functions $\tilde{G}_{\rm eff}(k,z)$ and $\eta(k,z)$.

III. LARGE-SCALE STRUCTURE OBSERVATIONS

We will assume that the background expansion rate is determined by a set of observations: type Ia supernovae, baryon acoustic oscillation (BAO), and other probes at low redshift and the CMB and nucleosynthesis at high redshift. These observations measure the luminosity or angular diameter distance at a given redshift. The distance measures in a spatially flat universe are, within factors of $1+z$, simply the comoving coordinate distance:

$$\chi(z) = \int_0^z \frac{dz'}{H(z')}. \tag{20}$$

Furthermore, BAO can directly measure the Hubble constant at the redshift of galaxies.

We are interested in the constraints available on perturbed quantities. Hence we will consider observational probes of large-scale structure to constrain modified gravity scenarios. In nearly all cases we will be interested in scales in the range 1–10^3 Mpc. The MG theories of interest must modify gravity on horizon scales of order 10^4 Mpc; it is an open question how they transition to GR on very small scales to satisfy experimental constraints from solar system tests. We will assume that the MG theories of interest differ from GR over the observationally accessible scales.

The most stringent current tests of gravity come from laboratory and solar system tests and from binary pulsar observations; see [28] for a review. Interesting probes of gravity on sub-Mpc scales also exist: galaxy rotation curves, satellite dynamics, strong lensing observations of galaxies and clusters, and x-ray plus lensing observations of clusters (e.g., [29]). Modifications in gravity can affect the propagation of gravitational wave. Future gravitational wave experiments such as LISA can detect gravitational wave from distant supermassive black hole pairs in the coalescence phase and thus test this effect [30]. We will not consider these tests in this paper. We will restrict our attention to large-scale structure on scales where theoretical predictions can be made using linear or quasilinear perturbation theory.

A. Connection of observables to perturbation variables

In principle, observations of large-scale structure can directly measure four fundamental variables that describe the perturbed metric and (fluid) energy-momentum tensor: the two scalar potentials ψ and ϕ that characterize the metric, and the density and velocity perturbations specified by δ and θ. Next we discuss the prospects for different probes of these variables.

Sum of potentials $\psi+\phi$: Gravitational lensing in either the weak or strong lensing regime probes the sum of the metric potentials. We will consider the weak lensing shear (or equivalently the lensing convergence) power spectrum as the primary statistical discriminator of MG via lensing.

The spatial components of the geodesic equation for a photon trajectory $x^\mu(\lambda)$ (where λ parametrizes the path) are

$$\frac{d^2x^\mu}{d\lambda^2} + \Gamma^\mu_{\rho\sigma}\frac{dx^\rho}{d\lambda}\frac{dx^\sigma}{d\lambda} = 0. \tag{21}$$

For the metric of Eq. (1), this gives the following relation for the first order perturbation to the photon trajectory [generalizing, for example, from Eq. (7.72) of [31]]:

$$\frac{d^2x^{(1)\mu}}{d\lambda^2} = -q^2\vec{\nabla}_\perp(\psi+\phi), \tag{22}$$

where q is the norm of the tangent vector of the unperturbed path and $\vec{\nabla}_\perp$ is the gradient transverse to the unperturbed path. This gives the deflection angle formula

$$\alpha_i = -\int \partial_i(\psi+\phi)ds, \tag{23}$$

where $s = q\lambda$ is the path length and α_i is the ith component of the deflection angle (a two-component vector on the sky). Since all lensing observables are obtained by

taking derivatives of the deflection angle, they necessarily depend only on the combination $\psi + \phi$ (to first order in the potentials).

For weak lensing tomography we use the shear power spectrum for two sets of source galaxies with redshift distributions centered at z_i and z_j. Following standard treatments of weak lensing, this may be derived from the deflection angle formula to get the shear power spectrum on angular wave number l ([32]):

$$C_{\gamma_i\gamma_j}(l) = \int d\chi W_i(\chi) W_j(\chi) k^4 P_{\psi+\phi}\left(k = \frac{l}{\chi}, \chi\right), \quad (24)$$

where the weight function W_i is simply

$$W_i \propto \frac{\chi_i - \chi}{\chi_i} \quad (25)$$

for source galaxies at a single comoving distance $\chi_i \equiv \chi(z_i)$ (it can be easily generalized for sources specified by a redshift distribution). We have assumed a flat background geometry for simplicity; our results throughout this paper can be generalized to a curved spatial geometry by replacing χ in the argument of W by the angular diameter distance.

Note that in the literature the lensing power spectra for GR are expressed in terms of the density power spectrum $P_\delta(k)$ assuming the standard Poisson and Friedmann equations. Usually anisotropic stress is neglected so that one can substitute into the above equation the relation between the power spectra: $P_{\psi+\phi} = 9k^{-4}H_0^4\Omega^2 P_\delta/a^2$ from Eq. (18). For MG, this substitution breaks down due to the modifications of the Poisson equation and the Friedmann equation. However the correct substitution can be made in terms of $\tilde{G}_{\rm eff}(k, z)$ using Eq. (19) and the modified Friedmann equation (which depends on the specific theory).

Since lensing probes the sum of the metric potentials, with the deflection angle formula following from the geodesic equation (which simply describes how curvature affects trajectories), it may not by itself test the field equations of the gravity theory. However lensing measurements at multiple source redshifts are sensitive to the growth of the lensing potential, which does offer a test of the MG theory. And by combining lensing with other observables, the relation of $P_{\psi+\phi}$ to P_δ can be tested. Recent studies that have examined constraints on MG theories with weak lensing include [18,33–39].

Another important observable in lensing is galaxy–galaxy lensing, the mean tangential shear around foreground (lens) galaxies. Its Fourier transform, the galaxy-lensing cross spectrum, depends on $\psi + \phi$ and on the galaxy number density. It is given by an equation similar to Eq. (24), with the power spectrum of the lensing potential in the integrand replaced by the three-dimensional cross-power spectrum, and with one of the weight functions replaced by one representing the foreground galaxy distribution:

$$C_{g_i\gamma_j}(l) = \int d\chi \frac{W_{gi}(\chi) W_{\gamma j}(\chi) k^2}{\chi} P_{g(\psi+\phi)}\left(k = \frac{l}{\chi}, \chi\right), \quad (26)$$

where W_{gi} is the normalized (foreground) galaxy redshift distribution (e.g., [40]). Galaxy–galaxy lensing has been well measured from the Sloan Digital Sky Survey (SDSS). It is a very useful check on galaxy bias; hence it aids the interpretation of galaxy clustering measurements ([41]) as well.

Assumptions: In using weak lensing observations with the above formalism, one assumes that intrinsic correlations are negligible or removable (in general these can differ for different gravity theories), that the weak lensing approximation is valid, and that galaxy properties that affect photometric redshift determination are not affected by the gravity theory.

Newtonian potential ψ: This can be measured by dynamical probes, typically involving galaxy or cluster velocity measurements. If gravity is the only force determining galaxy accelerations at large scales (as expected), we have from Eq. (10):

$$k^2\psi = \frac{d(a\theta_g)}{dt}, \quad (27)$$

where $\theta_g \equiv \nabla \cdot \mathbf{v}_g$. On sub-Mpc scales this relation can be used to constrain ψ using galaxy satellite dynamics and rotation curves (e.g., [42]). Redshift distortion effects in the galaxy power spectrum probe larger scales, which we address in more detail here.

The redshift space power spectrum of galaxies is a well-measured quantity. It can be expressed in the large-scale, small angle limit as (e.g., [43])

$$P_g^s(k) = \left[P_g(k) + \frac{2u^2}{H} P_{g\theta_g}(k) + \frac{u^4}{H^2} P_{\theta_g}(k)\right] F\left(\frac{k^2u^2\sigma_v^2}{H^2(z)}\right), \quad (28)$$

where $u = k_\parallel/k$ is the cosine of the angle of the $\mathbf{k}$ vector with respect to radial direction; P_g, $P_{g\theta_g}$, and P_{θ_g} are the real space galaxy power spectra of galaxies, galaxy-θ_g and θ_g, respectively; σ_v is the 1D velocity dispersion; and $F(x)$ is a smoothing function, normalized to unity at $x = 0$, determined by the velocity probability distribution. The dependence on u enables separate measurements of all three power spectra, though P_{θ_g} is the hardest to measure with high precision [44,45]. Furthermore, measurements of P_g^s at smaller scales provide information on pairwise velocity dispersion σ_v [46].

In the linear regime, we can rewrite Eq. (27) as

$$k^2\psi = \frac{d(aD_\theta)/dt}{D_\theta}\theta_g. \quad (29)$$

Here D_θ is the growth factor of θ_g. For MG models, D_θ has

a simple relation to D, the linear density growth factor: $D_\theta \propto a\dot{D} = a\beta HD$, where $\beta \equiv d\ln D/d\ln a$. In the linear regime we have $\theta_g(\mathbf{k}, t) = \theta_g(\mathbf{k}, t_i)D_\theta(\mathbf{k}, t)$. Note that the above equation does not require D_θ to be scale independent, so it is applicable to modified gravity models and clustered dark energy models. Note also that we do not distinguish the growth factor of θ_g from that of θ because we only use its time (redshift) derivative, which is expected to be very similar. Velocity measurements at multiple redshifts are required to measure ψ from the above equation, as described in [47].

For clustered DE models, the galaxy v_g is not necessarily equal to v of the total fluid. From the Euler equation (6) applied separately to different components of the fluid, we can see that the DM and DE velocities evolve differently since only the latter is affected by pressure perturbations in the DE. As a first order approximation, galaxies and baryonic gas velocities trace that of the DM. So what one actually measures is $\theta_g \simeq \theta_{\rm DM} \neq \theta_{\rm DE} \neq \theta$. This distinction can be relevant for DE models with large perturbations on subhorizon scales if these are not correlated with the matter fluctuations (i.e., if the DE power spectrum has a different shape from the matter power spectrum).

Assumptions/caveats: The galaxy peculiar velocity only probes ψ where there are galaxies. So potentially there is a bias related to the environment of galaxies. However, since gravity is a long range force, the potential where galaxies reside is determined by matter over a much larger region and thus should be unbiased with respect to the overall ψ. Galaxies themselves are not sufficiently massive to contribute to this long range potential. However, to obtain $\dot{v}_g$ from limited redshift bins, one does need to parametrize the redshift dependence of v_g.

The accuracy of the velocity information inferred from the redshift space galaxy power spectrum relies on the modeling of the redshift distortion. The derivation of Eq. (28) is quite general—it can be applied to general DE or MG models. However, Eq. (28) does not describe redshift distortions to percent-level accuracy [43]. Nonetheless, with improved modeling of the correlation function in redshift space [48] the associated systematic errors in velocity (and ψ) measurements can be reduced.

Density contrast δ: The clustering of galaxies is one of the earliest measures of large-scale structure, and its measurements have advanced over the last three decades. The galaxy power spectrum P_g is the simplest statistical measure of correlations in the galaxy number density. Several other probes of large-scale structure also probe the density field: clustering of the Lyman-alpha forest, clustering of quasars and galaxy clusters, the abundance of galaxy clusters, and (in the future) 21-cm emission measurements of the high-redshift universe.

However, given a measured galaxy power spectrum, the power spectrum P_δ of the underlying mass density δ may differ due to galaxy bias. Further the galaxy-density relation may be nonlocal and vary slightly in different gravity theories due to differences in the tidal field that influence collapsed objects such as galaxy halos. We will restrict ourselves to large scales ($k \ll k_{\rm nl}$, the nonlinear wave number) where bias is scale independent in simple models of galaxy formation. This allows us to infer the mass power spectrum from the galaxy power spectrum without detailed modeling of their relation, because it is possible to fit for the bias directly from the data. We discuss below the caveats to this assumption for clustered dark energy.

The galaxy density in three-dimensional space may be expressed in terms of the density and bias parameters b_1 and b_2 as

$$\delta_g \equiv \frac{\delta n_g}{n_g} = b_1\delta + \frac{b_2}{2}\delta^2. \tag{30}$$

This expansion is useful for small values of δ; it can be used in a perturbative expansion to explore what measurements are sufficient to measure the bias parameters b_1, b_2 as well as δ (see [49] for details on the bias formalism). Equation (28) shows how the three-dimensional galaxy power spectrum P_g can be obtained from redshift space measurements. A second way of measuring P_g is from imaging data with photometric redshifts. This provides measurements of the angular power spectrum of galaxies, which is a projection of the three-dimensional galaxy power spectrum

$$C_g(l) = \int d\chi \frac{W_g^2(\chi)}{\chi^2} P_g\left(k = \frac{l}{\chi}, \chi\right), \tag{31}$$

where W_g is the normalized redshift distribution of galaxies included in the sample. With good photo-z's it is a narrow range with width of order 0.1 in redshift, so that many such angular spectra can be measured at different mean redshifts from a survey (e.g., [50]).

1. Galaxy bias with clustered dark energy

In clustered dark energy models it is not *a priori* clear whether the galaxy overdensity is related to the matter overdensity δ_m or to the total fluid overdensity $\delta_{\rm GR}$. We argue below that at least for some galaxy populations, δ_g is directly related to δ_m, even though the evolution of the matter density responds to the full gravitational potential (which receives contributions from dark energy clustering as well).

One way to see this is to consider the centers of mass of galaxy halos at sufficiently high redshift z_i where the dark energy density is negligible. The clustering of these halo centers is then simply a biased version of the mass distribution. Hence at z_i one can write $\delta_g(z_i) = b(z_i)\delta_M$, with $b(z_i)$ independent of scale for large enough scales. As they evolve to redshifts below unity, their motions are given by the potential ψ, just as for the matter field. Hence their

evolution obeys the continuity and Euler equations: $\dot{\delta}_g \simeq -\theta_g/a$ and $\dot{\theta}_g \simeq -H\theta_g + k^2\psi/a$. The matter density obeys the same equations with δ_M and θ_M as the density and velocity perturbations. This means that the bias factor preserves its scale independence: at low redshift, it relates the galaxy power spectrum to the matter power spectrum and is not directly sensitive to the clustering of dark energy. For example the halo-model expression [51,52] for the bias evolution is $b(z) \simeq 1 + (\nu - 1)/\delta_{\rm sc}(z)$, where $\delta_{\rm sc}(z) \propto D(z)$ is the density required for spherical collapse at z, and $\nu \equiv \delta_{\rm sc}(z)/\sigma$ with σ the smoothed rms mass fluctuation. The expression for ellipsoidal collapse has two additional parameters but still has no scale dependence.

Clustered dark energy follows Eq. (6) with $w \neq 0$ and $\sigma \neq 0$, so it has a different time and spatial dependence from δ_m. If the dark energy clusters significantly, it is therefore possible that galaxies have a scale dependent bias relative to it and therefore to the total density field.

The above argument is very general but relies on some approximations. These are well justified for massive halos, for which the evolution at low redshift is very simple: consider galaxy halos of mass $M \gg M_*$, where M_* is the standard halo-model nonlinear mass. The centers of mass of these halos can be mapped to high-σ peaks in the nearly Gaussian mass distribution at high redshift. Moreover, they do not move significantly, so it is evident that their power spectrum at large scales evolves simply by the growth of its amplitude. Such massive halos correspond to galaxy clusters and luminous red galaxies (LRGs) at moderate to high-redshift. For galaxies in lower mass halos, halo motions and mergers change their clustering at low redshift, so one has to be careful in modeling their bias factors.

Another route to δ in any GR scenarios is through the metric potentials. Given lensing measurements of $\psi + \phi$ and dynamical measurements of ψ, one can obtain the potential ϕ. Using this, the Poisson equation (7) then gives δ, since the gravitational constant is known in GR. Thus δ is not independent of the metric potentials even for clustered DE models.

2. Empirical determination of bias

To leading order then, knowledge of b_1 allows us to relate P_g to P_δ. Barring extreme scenarios of clustered dark energy, we take δ to be the full density field.

Provided a halo-model description applies reasonably well to our universe, bias can be determined by combining observations and using two- and three-point statistics. For concreteness we consider the bias parameters b_1, b_2 that can be determined from the data using the power spectrum and bispectrum (denoted B) measurements. In a deterministic bias model, one can then get the density power spectrum. With $P_g = b_1^2 P_\delta$ and the reduced three-point parameter $Q \sim B/P^2$ (see the Appendix and [49] for full expressions), one has a relationship between the Q parameter of galaxies and mass [53,54]:

$$Q_g = \frac{Q_\delta}{b_1} + \frac{b_2}{b_1^2}. \tag{32}$$

By using P_g and measurements of Q_g for different triangles, both bias parameters and P_δ can be determined. (A similar analysis can be done in real space, e.g., using counts in cells. The skewness S_3 is given by the shape of the power spectrum and bias parameters.) While this is a simplified model, it helps us address what changes for MG: the predictions for P_δ and Q_δ both change, with the former given by the new linear growth factor on large scales and the latter by next order terms in perturbation theory (see the Appendix for more details). For well-specified gravity scenarios, these calculations can be done and thus the bias factors determined from measurements.

A second approach to measuring b_1 is to use the galaxy-mass cross correlation measured by galaxy–galaxy lensing in combination with the galaxy power spectrum (e.g., [41]). This has the advantage that one uses only two-point statistics that can be measured with high accuracy. However, as discussed below and by [25], for MG theories there is a complication because the Poisson equation is needed as well since lensing measures the potentials rather than δ. So for MG theories, the extraction of the bias parameter in this approach is more complicated, but nevertheless feasible by jointly fitting for bias and $\tilde{G}_{\rm eff}$.

3. Galaxy cluster mass function

A different probe of δ is provided by *the mass function of galaxy clusters*. Given Gaussian initial conditions and a spherical/ellipsoidal collapse model, the number density of galaxy clusters can be related to the linear density contrast. In the spherical collapse scenario, a region containing mass M will collapse if the overall density fluctuation exceeds a threshold δ_c. The number of such regions can be predicted from the Gaussian statistics and this fixes the halo mass function dn/dM, the number of halos with mass M.

In the standard ΛCDM cosmology, gravitational dynamics is determined by GR. The mass function of galaxy clusters is sensitive to the smoothed mass density variance σ_R^2 on scale R, which is dependent on the cluster mass and is typically of order 10 Mpc (e.g., [55]). This is related to the density power spectrum as

$$\sigma_R^2 = \int \frac{d^3k}{(2\pi)^3} P_\delta(k) W_{\rm top\ hat}^2(kR), \tag{33}$$

where $W_{\rm top\ hat}$ is the window function for averaging with a spherical top hat.

For clustered DE models, the cluster formation picture becomes complicated. The presence of the anisotropic stress invalidates the spherical collapse model and more complicated models such as ellipsoidal collapse with tidal fields need to be used. Furthermore, the fate of an overdense region is no longer determined by the matter fluc-

tuation δ_m alone. DE fluctuations $\delta_{\rm DE}$ and σ affect ψ through Eqs. (7) and (8). And δp affects the evolution of $\delta_{\rm DE}$ through Eqs. (5) and (6). Thus a combination of δ_m, $\delta_{\rm DE}$, δp, and σ acts in determining the evolution of a given region of matter—the resulting collapse condition has yet to be worked out. Since many galaxy clusters form recently at $z \lesssim 1$, where DE is non-negligible, DE fluctuations could leave some detectable signatures in cluster abundance.

For probing the dark universe, this is a valuable feature. It implies that galaxy cluster abundances contain information on not only fluctuations in matter but also fluctuations in dark energy, and thus is a promising probe of the total δ. To extract such information requires further modeling of the DE model, but a simplified model can be obtained as follows. The collapse condition based on energy conservation should be linear in the DM and DE perturbation variables, since they are all first order variables of the energy-momentum tensor. At high redshift, the dark energy contribution should vanish (assuming $\bar{\rho}_{\rm DE} \ll \bar{\rho}_m$). Thus we may assume that matter fluctuations are the only source of growth for the late time δ_m as well as $\delta_{\rm DE}$, δp, and σ responsible for the LSS. In this picture, all perturbation variables are correlated and have deterministic relations [56]. The collapse condition can be simplified into a modified condition on δ_m alone. An effective $\delta_c^{\rm eff}$ can be defined for specific DE models, such that when a region reaches $\delta_m \geq \delta_c^{\rm eff}$, it will collapse.

The usual collapse model deals with isolated objects and thus Birkhoff's theorem is implicitly required. Modifications in GR result in a generic breakdown of Birkhoff's theorem. This significantly complicates the modeling of cluster abundance in MG models, since the fate of a given region is determined not only by matter and energy inside this region, but also matter and energy outside. However, given a MG model, one can still predict the probability for a given region with overdensity δ_m to collapse and thus predict cluster abundances.

Assumption/caveats: Unlike the use of gravitational lensing to probe $\psi + \phi$, it is model dependent to probe δ from cluster abundance. (1) The cluster abundance requires careful modeling, even in the simplest case of smooth DE models. For example, the tidal field makes the spherical collapse model only a rough approximation. (2) The observable-mass relation is needed to connect observable [e.g., x-ray flux, Sunyaev Zel'dovich (SZ) flux, or cluster richness] to the mass of clusters. These cluster properties often involve complicated gastrophysical processes and cannot be predicted with sufficiently high precision from first principles. As a consequence, using cluster abundance to probe δ often requires model-dependent calibrations.

In spite of these caveats, it is hoped that the well-posed problem of the evolution of a region in an initially Gaussian random field will be calculable and related to the linear density field in generic MG or DE models.

Velocity divergence θ: Many existing velocity measurements are based on distance indicators: the difference of the true distance from what is inferred from the recession velocity gives an estimate of the peculiar velocity of a sample of galaxies or clusters [57]. The pairwise velocity at small separation can be measured through anisotropic galaxy clustering in redshift space at cosmological distances [46]. While challenging, there are ongoing attempts to improve measurements of bulk flow measurements, based on SNe Ia [58]. An independent method is the kinetic SZ effect [59] of clusters which is directly proportional to the cluster peculiar velocity and enables a rather model-independent measurement method [60]. These measurements are likely to have lower signal-to-noise ratio than the redshift space distortions discussed above. Further it is unclear whether they estimate θ of the total fluid in a clustered DE scenario, for the reason discussed above.

CMB: The CMB power spectrum is given by

$$C_{TT}(l) = \int dk \int d\chi' F_{\rm CMB}(k, l, \chi') j_l[k\chi(z')], \qquad (34)$$

where the spherical Bessel function j_l is the geometric term through which the CMB power spectrum depends on the distance to the last scattering surface. The function $F_{\rm CMB}$ combines several terms describing the primordial power spectrum and the growth of the potential. We will regard $F_{\rm CMB}$ as identical to the GR prediction since we do not invoke MG in the early universe (up to the redshift at last scattering).

The CMB anisotropy does receive contributions at redshifts below last scattering, in particular, due to the integrated Sachs-Wolfe (ISW) effect [61]. In the presence of dark energy or due to modifications in gravity, gravitational potentials are in general time varying and thus produce a net change in the energy of CMB photons:

$$\frac{\Delta T}{T}\bigg|_{\rm ISW} = -\int \frac{d(\psi + \phi)}{dt} a(t) d\chi. \qquad (35)$$

The ISW effect, like gravitational lensing, depends on and probes the combination $\psi + \phi$. The ISW signal is overwhelmed by the primary CMB at all scales (although it does produce a bump at the largest scales in the CMB power spectrum). For this reason, it has to be measured indirectly, through cross correlation with other tracers of large-scale structure. The resulting cross-correlation signal is then

$$C_{\rm ISW}(l) = \int P_{g(\dot{\psi}+\dot{\phi})}\left(k = \frac{l}{\chi}, \chi\right) a^2 \frac{d\chi}{\chi^2}. \qquad (36)$$

Here, $P_{g(\dot{\psi}+\dot{\phi})}(k, \chi)$ is the cross-power spectrum of $(\dot{\psi} + \dot{\phi})$ and galaxies or other tracers of the LSS such as quasars or clusters. By cross correlating the CMB temperature with galaxy overdensity δ_g, the ISW effect has been detected at $\lesssim 5\sigma$ confidence level [62] and provides independent evidence for dark energy, given the prior of a spatially

flat universe and GR. This cross-correlation signal depends on galaxy bias, which has to be marginalized to infer cosmology. With the aid of gravitational lensing, uncertainties of galaxy bias can be avoided [63,64]. Furthermore, since the ISW amplitude peaks on the largest scales, it also has a strong correlation with large-scale bulk flows and produces a cross-correlation signal with potentially better signal-to-noise ratio than that of the density-ISW cross correlation [65].

The primary CMB is Gaussian and statistically isotropic. However, gravitational lensing distorts the CMB sky and induces anisotropy and Fourier mode coupling in the CMB, which should not exist otherwise. This feature allows reconstruction of the lensing potential from future high resolution CMB maps [66]. The CMB sky is the furthest lensing source and thus can probe $\psi + \phi$ at redshifts well above unity. This will be useful to constrain those MG and DE models in which deviations from ΛCDM persist at these redshifts.

ISW measurements and future measurements of lensing and galaxy clustering can probe scales approaching the horizon scale. This provides an additional test of MG models in which the growth of perturbations is altered at relatively high redshift on superhorizon scales. Bertschinger [23] showed that growth on superhorizon scales is constrained to be universal for MG models with $\psi = \phi$. Hu and Sawicki [24] showed how it differs for $f(R)$ models which do not obey this constraint, and describe the transition from superhorizon to subhorizon scales. If measurements achieve high accuracy on these large scales, they can be combined with information on subhorizon scales to provide additional constraints on the ratio of potentials η for such MG models.

Summary: The quantity that can be measured most robustly is the sum of potentials $\psi + \phi$, through gravitational lensing and the ISW effect. With a bit more modeling, the Newtonian potential ψ can be inferred from galaxy velocity measurements (i.e., redshift space distortions). To obtain model-independent constraints on the total density perturbation δ is challenging if one allows for dark energy clustering in the GR scenario. Galaxy clustering is likely to be an effective measure of the matter fluctuation δ_m, while cluster abundance is a promising probe of δ as it is sensitive to DE fluctuations as well. Although the galaxy peculiar velocity is likely to be well measured in the future, the DE peculiar velocity (and therefore the overall v and θ) is likely the most difficult to measure. Cross correlations of large-scale structure tracers with the lensing potential or the Newtonian potential are probably the most promising tests of MG in the near future, as we discuss next.

B. Joint constraints from multiple observations

If multiple observables are to be combined, model-independent information can only be inferred if they probe the same range of redshift and length scale. The distance-redshift relation will be measured to $\sim 1\%$ accuracy by the next-generation SNIa and BAO surveys at low-z and by the CMB at high-z. The next-generation BAO surveys can further measure $H(z)$ at low redshift. With the expansion rate of DE and MG models tightly constrained, measurements of perturbed variables become powerful discriminators.

The distance-redshift relation at redshift z is given by an integral over the expansion rate, and therefore the energy densities, from redshift 0 to z. This measurement at $z \lesssim 1$ has provided evidence of acceleration, consistent with ΛCDM. On the other hand, CMB measurements at high-z for both distances and perturbations are consistent with a universe governed by GR, with its energy density dominated by matter and radiation [40]. Thus either dark energy or modification of gravity must produce effects that are significant at $z \lesssim 1$ and negligible at $z \sim 1000$. In Fig. 1 we show as examples the deviation (from ΛCDM with $\Omega_{\rm DE} = 0.7$) of a model with $\Omega_{\rm DE} = 0.75$ and a flat DGP model with $\Omega_m = 0.3$. It is clear that for both dis-

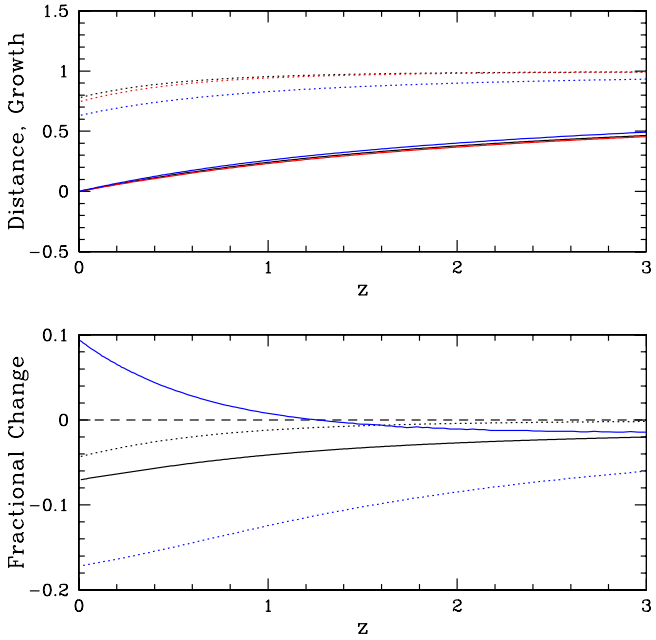

FIG. 1 (color online). Upper panel: We plot the normalized distance $d(z)$ (solid curves, almost coincident) and the linear growth rate $D(z)/a(z)$ (dotted curves) for $0 < z < 3$ for two dark energy models (in black and red) and a DGP model (in blue). The distances and growth rates are normalized to give 1 at high redshift ($z = 1100$). Lower panel: The fractional deviations in distance (solid curves) and linear growth (dotted curves) from the fiducial ΛCDM model are shown for a dark energy model (black) and DGP (blue) (see text for details). Note that the DGP growth curve is sensitive to the parameters chosen to fit the distance-redshift relation: for a distance curve that matches ΛCDM better, the growth curve would also have smaller deviation.

tances and perturbations, significant deviations occur at low-z in such models [67].

The most promising scale/redshift range in the near future is $\sim$10–100 s Mpc at redshifts $\sim$0.3–1. Imaging and spectroscopic observations are likely to be made on these scales and will be robust to many sources of error and dependence on specific models. We list below several categories of surveys that will test MG and DE models. Two sets of surveys are indicated: surveys planned for the near future (significant data within 5 years), and surveys planned to start in about a decade. (The list is not complete as several projects have been formulated or modified recently.)

(1) Multicolor imaging survey: With photometric redshifts for millions of galaxies, these surveys provide measurements of weak lensing, galaxy cluster abundances, and the angular clustering of galaxies, clusters, and quasars. These measurements probe $\psi + \phi$, δ_g and their cross correlation. Upcoming surveys include the following:

(a) DES, KIDS, PS1, HSC (2008–). $0 < z \lesssim 1$.

(b) LSST, SNAP, DUNE (2014–). $0 < z \lesssim 3$.

(2) Spectroscopic surveys: While primarily designed to measure the distance-redshift relation and $H(z)$ using the baryon acoustic oscillations in galaxy power spectra, they will provide improved measurements of P_g, P_{gv}, and P_{vv} on large scales. Some surveys will target $z \lesssim 1$ galaxies and others will select galaxies at higher redshift, $2 \lesssim z \lesssim 3$.

(a) LAMOST, WiggleZ, HETDEX, WFMOS, BOSS (2008–). $0 < z \lesssim 3$.

(b) ADEPT (2014–). $1 \lesssim z \lesssim 2$.

(3) 21 cm surveys: SKA [68] (2015–). The square kilometer array (SKA) has the potential to detect $\sim 10^9$ galaxies over $0 < z \lesssim 1.5$, with a deeper survey extending to $z \sim 5$, through 21 cm line emission of neutral hydrogen in galaxies. If successful, it will provide high precision measurements of the distance-redshift relation through BAOs [69], and tests of MG through (a) weak lensing maps with accuracy comparable to that of large optical surveys [70], (b) velocity measurements through redshift distortions of galaxy clustering [25], and (c) ISW measurements through CMB-galaxy cross correlations.

(4) SZ and x-ray cluster surveys: These will measure the abundances of galaxy clusters out to $z \sim 1$ and beyond. Cosmological applications will depend on supplementary optical data to get photometric redshifts of the detected clusters.

(a) SZA, SPT, ACT, APEX, eROSITA (2008–). $0 < z \lesssim 1$.

(5) CMB: temperature and polarization maps provide high-z constraints and also measurements of the ISW effect and CMB lensing, which are probes of $\psi + \phi$ at lower redshift.

(a) PLANCK and ground based missions (2008–).

We have indicated the approximate redshift range over which these surveys will provide accurate measurements. It would be most useful to have different observables overlap in redshift and length scale in the range $z \simeq 0.3$–1 and at scale $\lambda \simeq 10$ to several 100 Mpc. This range of scales covers the linear and quasilinear regimes of structure formation (we are assuming that MG effects are present on these scales). Next we consider two promising combinations of observables that on the 5–7 yr time scale will enable measurements of the MG functions $\tilde{G}_{\rm eff}$ and η on these scales.

Lensing and galaxy power spectra: Planned next-generation imaging surveys (see above) will have area coverage in excess of 1000 sq. degrees, enabling a few percent-level measurements of lensing power spectra. The same imaging surveys will also measure the angular clustering of the galaxies C_g (at $z \sim 0.3$–0.6, the redshift of the lensing mass) to percent-level accuracy; cluster abundances will also be measured through optical and SZ surveys: both measurements probe the matter density δ. Alternatively, spectroscopic surveys like BOSS will measure P_g, the three-dimensional power spectrum, to percent-level accuracy. The shear power spectra can be combined with the density power spectra measured at $z \sim 0.3$–0.6 and scales of 10–100 Mpc. Using the Poisson equation, $\tilde{G}_{\rm eff}$ will then be tightly constrained, assuming statistical errors dominate the error budget. The main galaxy sample and LRG sample of the SDSS has already been used in constraining MG models through galaxy clustering alone (e.g., [71]), though in a model-dependent way.

Cross correlations of galaxies with shear and velocity: Galaxy–galaxy lensing measurements made from imaging surveys probe the lensing potential-galaxy correlation. This measurement has been made to high accuracy from the SDSS [72,73]. In the near future one can expect measurements of P_{gv} to a few percent (e.g., from the BOSS survey) at $z \sim 0.3$–0.6. In combination with percent-level galaxy-galaxy-lensing measurements over the same range of redshift, the ratio of potentials η will be precisely constrained [47].

The measurements described above would be major advances in constraining MG theories, as the current constraints on $\sim$10–100 Mpc scales are weak and insufficient to test MG theories with any robustness. For particular models the scale and redshift evolution of a single statistic, such as the lensing power spectrum, can be powerful as well. We leave for future work a detailed study of how well these measurements will test MG theories. In considering an observable suitable for distinguishing models of gravity, one must address the familiar problems in extracting cosmological information due to statistical and systematic errors, i.e., the expected precision on the measurement, the physical assumptions necessary to connect observable to the four variables of interest, and the degeneracy with other cosmological parameters.

IV. MODIFIED GRAVITY VS DARK ENERGY

Specific models of MG and DE can be tested by combining observations of the expansion rate and large-scale structure. For example, in the ΛCDM model (and well-defined scalar field models), the growth of the large-scale structure is completely determined by the expansion history: there exists a fixed relation between the expansion rate and the growth of LSS. This consistency check has been carried out in the literature and is indeed able to distinguish specific models investigated [10]. Furthermore, this consistency check can be performed in a model-independent way to search for signatures of violation of GR, with the prior of smooth DE [74–76].

DE models that depart from scalar field models can be much more complicated, with a breakdown of the correspondence between the expansion rate and large-scale structure. The expansion rate is determined by $\bar{\rho}_{\rm GR}$ and w. However, two extra DE properties, the anisotropic stress σ and the response of pressure to perturbations (δp), can affect the growth of the LSS. These two properties are determined by the microphysics of the DE model and are independent of $\bar{\rho}_{\rm GR}$ and w. As a consequence, the growth of LSS is no longer fixed by the expansion rate and the above consistency check cannot be applied to search for signatures of the violation of GR. Current observational constraints on the sound speed ($c_s^2 \equiv \delta p/\delta\rho$) [77] and the anisotropic stress [78] are weak. Furthermore, these studies use a particular form of σ and δp and assume that one can be switched off when studying the other. Thus a potentially wide range of DE models with non-negligible anisotropic stress and pressure fluctuations are still viable against observations. To investigate the feasibility of distinguishing between DE and MG, we will allow for arbitrary anisotropic stress and pressure perturbations.

Modifications of gravity (at least the class of theories we have considered) involve two extra quantities which govern LSS, namely, modification of Newton's constant, $\tilde{G}_{\rm eff}$, and the ratio of potentials $\eta \equiv \phi/\psi$. Although these quantities determine the gravitational interaction of perturbations, they do in general affect the expansion rate $H(z)$—unlike for GR and its Newtonian limit. This is in part due to the fact that for MG, Birkhoff's theorem no longer holds and thus the usual exercise of calculating $H(z)$ from the Newtonian dynamics of a spherical matter distribution no longer applies. Thus $\tilde{G}_{\rm eff}$ and η represent real extra degrees of freedom in MG theories.

The extra degrees of freedom in MG and clustered DE models can produce similar observational consequences. For example, the anisotropic stress breaks the equality between ϕ and ψ, mimicking the role of η in MG models. Thus one might expect that by tuning the 2 extra degrees of freedom in DE models, one can mimic a given MG model to fit observations. Indeed, Kunz and Sapone [19] explicitly construct a DE model which reproduces degenerate ϕ, ψ, and δ_m with the flat DGP modified gravity model [79].

This degeneracy certainly deserves further investigation. In this section, we consider in more detail the question: can one always succeed in tuning DE models to produce observational consequences identical to a given MG model? If the answer is yes, then one can never unambiguously test for deviations from GR.

The answer to the above question is incomplete in fully describing the dark degeneracy. The complementary question, which needs to be answered is: can one always tune MG models to produce observational consequence identical to a given DE model? If the answer is yes, then one can never unambiguously justify the existence of DE. However, this question is more difficult since it requires a general parametrization of the relation between the expansion rate $H(z)$ and the nature of a general gravity theory—such a parametrization is not yet available. This limit in theoretical understanding of MG forces us to investigate only the first question, since we know the most general way of parametrizing the influence of DE on the expansion history of the Universe. Furthermore, we have constrained our study to a special class of MG models, in which gravity is minimally coupled to matter. The study of both questions for the most general MG models is beyond the scope of this paper.

The relationship between the four perturbation variables ϕ, ψ, δ, and θ is fixed for a complete DE or MG theory. These consistency relations are the key to probing the nature of DE and MG. With just two variables being observable, one can only test against one consistency relation and, as we see below, by tuning the 2 extra degrees of freedom in clustered DE models, any MG model can be mimicked. However, with more observed variables, one can test other consistency relations and hope to break the degeneracy between DE and MG models. In this section, we explore the feasibility of distinguishing DE and MG models. In this section we consider only the question of distinguishability in principle, without regard to the accuracy of observations in the foreseeable future.

A. Two perturbation observables

First we assume that both potentials are observables, i.e., we require ϕ and ψ to be identical in the two models. From the discussions in previous sections, these two quantities are the most likely to be measured to high precision. So we set them identical in the constraint equations for GR and MG to get relations between the remaining variables. Comparing Eq. (8) for σ in GR with the constraint Eqs. (12) and (13) for MG gives

$$\sigma = \frac{2}{3}\frac{\eta^{-1}-1}{\eta^{-1}+1}\frac{\tilde{G}_{\rm eff}}{G}\frac{\bar{\rho}_{\rm MG}}{\bar{\rho}_{\rm GR}}\delta_{\rm MG}. \tag{37}$$

In addition by combining the Poisson equation (7) for GR with Eqs. (12) and (13) for MG, we obtain a second constraint

$$\delta_{\rm GR} + 3(1+w)Ha\frac{\theta_{\rm GR}}{k^2} = \frac{2}{\eta^{-1}+1}\frac{\tilde{G}_{\rm eff}}{G}\frac{\bar{\rho}_{\rm MG}}{\bar{\rho}_{\rm GR}}\delta_{\rm MG}. \quad (38)$$

The question then is whether Eqs. (5), (6), and (38), have solutions for $\delta_{\rm GR}$, $\theta_{\rm GR}$, and δp, in terms of MG variables [recall that σ is now fixed by Eq. (37)]. Without a fundamental theory, δp can take any form [21]: hence there is *always* a form of δp satisfying all three equations. Namely, there is always a DE model which can mimic the given MG model to produce identical ϕ and ψ.

The degeneracy persists for other combinations of two perturbation variables. We have discussed above that in a clustered DE model, it is difficult to establish whether galaxies, other tracers, or cluster abundances probe δ or δ_m (or neither). If we assume that a subset of LSS observations will provide measurements of δ, then combining that with measurements of $\psi+\phi$ from lensing, we have

$$\sigma = \frac{2}{3(1+w)}\delta\left(\frac{\tilde{G}_{\rm eff}\bar{\rho}_{\rm MG}}{G\bar{\rho}_{\rm GR}} - 1\right). \quad (39)$$

Thus if σ is free, it can be chosen to match the above equation for any set of theories.

Extra information can break this degeneracy. The response of pressure to density perturbations and the anisotropic stress are determined by the microphysics of the DE model. It requires a theory to provide such closure relations (see [24] for more detailed discussions). For example, the quintessence model predicts vanishing σ and negligible pressure perturbation on subhorizon scale. Even if advances in the understanding of general DE theory do not provide such specific information, some general constraints can still break the degeneracy. For example, if δp takes the form $\delta p = c_s^2\delta\rho$ and $c_s^2 = c_s^2(t)$, as is true for the adiabatic case, solutions do not exist in general for Eqs. (5), (6), and (38). In this case, one cannot find a DE model to mimic the given MG model.

Another physically well-motived example is for the anisotropic stress σ. A natural source of σ is the velocity perturbations in the fluid. By the requirement on gauge invariance, the evolution in σ may be parametrized in the following form in the Newtonian gauge [78,80]:

$$\sigma + 3H\dot{\sigma} = \frac{8}{3}\frac{c_{\rm vis}^2}{1+w}\theta, \quad (40)$$

where $c_{\rm vis}$ is the viscous parameter. This equation in general contradicts Eqs. (37) and (39) above and thus no DE model that satisfied Eq. (40) can mimic the given MG model.

Extra information can also come from additional observables. The equations above show that if we have just one additional observable, such as δ or θ, there will in general be no solution for the remaining two variables that satisfies three equations [e.g., (5), (6), and (38)]. We consider this next.

B. Three or more observables

If both potentials and δ are observable then the theory is constrained much more tightly, especially if they are measured multiple redshifts.

For a DE model to mimic the given MG model, δ, ϕ, and ψ must satisfy the three equations (7), (12), and (13). This imposes the following consistency relation for $\tilde{G}_{\rm eff}$ and η:

$$\eta^{-1} = 2\frac{\tilde{G}_{\rm eff}}{G}\frac{\bar{\rho}_{\rm MG}}{\bar{\rho}_{\rm GR}} - 1. \quad (41)$$

So if the given MG model does not obey the above relation, no DE model can produce δ, ϕ, and ψ identical to the given MG model, no matter how the DE properties are fine-tuned.

Equation (41) represents a strong constraint on MG models as it shrinks the 2-parameter $\eta - \tilde{G}_{\rm eff}$ space in MG models into a straight line. We show as an example that the DGP model does not satisfy this condition.

In a flat DGP model, $\tilde{G}_{\rm eff} = G$ and $\eta^{-1} = (1 + 1/3\beta_{\rm DGP})/(1 - 1/3\beta_{\rm DGP})$ [11]. Here $\beta_{\rm DGP} = 1 - 2r_cH(1+\dot{H}/3H^2) = 1 - 2r_cH/(1-2r_cH) < 0$, with $H^2 = H/r_c + \Omega_m a^{-3}$ and $r_c = 1/(1-\Omega_m)$. We have normalized $H(z=0) = 1$. For the DGP model, $\bar{\rho}_{\rm MG} = \Omega_m a^{-3}$ (up to a normalization, which is irrelevant for this discussion). By requiring the DE model to reproduce the expansion history of the given MG model, we have $\bar{\rho}_{\rm GR} = H^2$. Figure 2 shows that the consistency condition is significantly violated by all flat DGP models. This means that no DE model can produce ϕ, ψ, and δ identical to a flat DGP model that satisfies observational constraints on the expansion history.

This conclusion seems to contradict [19]. However, [19] requires the dark matter density fluctuation δ_m to be identical in the GR and MG scenarios. We require the total δ to be identical instead. In GR, the Poisson equation specifies the $\phi - \delta$ relation, not the $\phi - \delta_m$ relation, so with δ as an observable, one directly constructs consistency relations and thus distinguishes between DE and MG.

There is also a constraint on the anisotropic stress, from Eqs. (8), (12), (13), and (38),

$$\sigma = \frac{\eta^{-1}-1}{3(1+w)}\delta. \quad (42)$$

Comparing Eq. (6) with Eq. (10), we obtain

$$\theta\left(3Hw - \frac{\dot{w}}{1+w}\right) + \left(\frac{c_s^2}{1+w}\delta - \sigma\right)\frac{k^2}{a} = 0. \quad (43)$$

Since $H\theta \sim \beta aH^2\delta \ll k^2\delta/a$, we have

$$c_s^2 \simeq \frac{(1+w)\sigma}{\delta} = \frac{\eta^{-1}-1}{3}. \quad (44)$$

Comparing Eq. (5) with Eq. (9), we obtain

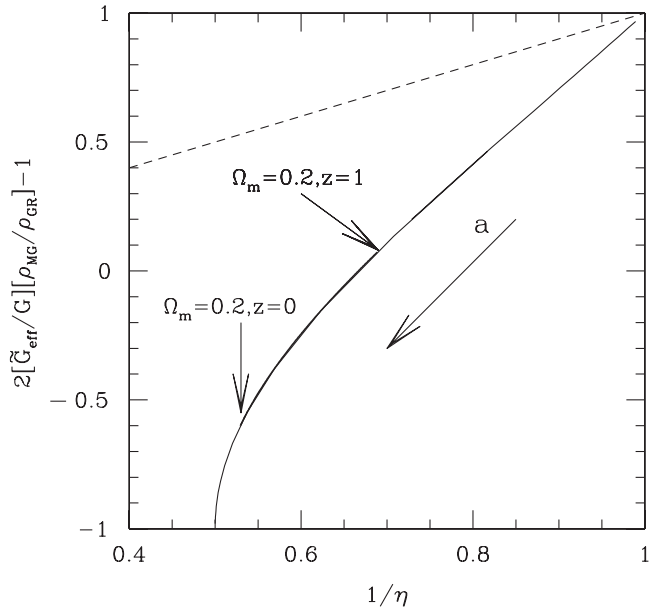

FIG. 2. First consistency condition for at least one DE model to mimic ϕ, ψ, and δ in a flat DGP model. The dashed line given by Eq. (41) represents the required condition, while the solid curve is the actual relation in flat DGP. When $a \to 0$, $\eta \to 1$ and for $a \to \infty$, $\eta \to 1/2$. The points on the curve with $a = 0.5$ and $a = 1$ are indicated. (For flat DGP lines with different Ω_m lie on top of each other.) The disagreement between the two curves shows that DGP is a modified gravity model that cannot be mimicked by any dark energy model.

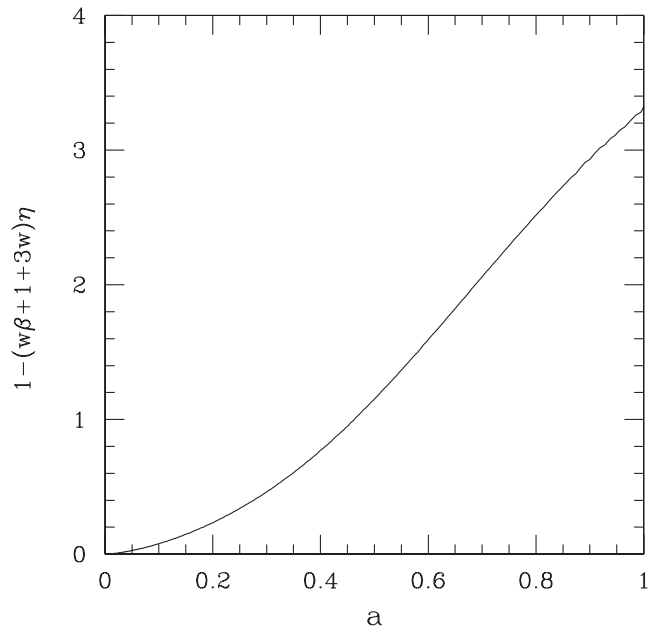

FIG. 3. The second necessary condition for at least one DE model to mimic ϕ, ψ, and δ in the given DGP model. The condition $\eta^{-1} \simeq w\beta + 1 + 3w$, given by Eq. (46) implies the variable on the y axis should be zero for all a. For flat DGP with $\Omega_m = 0.2$, this condition is also severely violated for $a > 0$.

$$c_s^2 = \frac{w(\theta/a - 3\dot{\phi})}{-3H\delta} + w \simeq w\left(\frac{\beta}{3} + 1\right). \quad (45)$$

Combining both constraints on c_s^2, we obtain

$$\eta^{-1} \simeq w\beta + 1 + 3w. \quad (46)$$

w is fixed by the condition $\bar{\rho}_{\rm GR} = H^2$. β is calculated from the given MG theory. So the above equation can be checked from the viewpoint of MG models unambiguously.

Again, Fig. 3 shows that this condition is severely violated for the DGP model: thus no DE model can mimic a flat DGP model to reproduce identical ϕ, ψ, and δ. We have verified that this is true for $f(R)$ models as well.

These relations present general constraints, without resort to real observation data. Observations show that at the present epoch, $w < -1/3$ since the universe is accelerating, while $\beta > 0$ since the structure is growing. From Eq. (45), we have $c_s^2 < -1/3$, if the related DE model can reproduce ϕ, ψ, and δ. Furthermore, Eq. (46) tells that $\eta < 0$ today.

V. DISCUSSION

We have described the role of perturbations in testing theories of MG against large-scale structure observations. We have chosen the class of MG theories that are described by scalar perturbations, so that two metric potentials suffice to describe the perturbed space-time. We then consider the quasistatic, Newtonian limit of the perturbed field equations and compare DE and MG theories.

Our main focus is on the relationship of different observables—lensing, large-scale dynamics of galaxies, galaxy clustering, cluster abundances, and various cross correlations—to the four perturbation variables of MG theories including the two metric potentials, the density field, and the divergence of the peculiar velocity. In Sec. III we give the relationship of measured power spectra in real space, redshift space, and on the sky with theoretical predictions for these perturbation variables. We highlight the use of two effective functions to test MG theories: the ratio of the metric potentials ϕ/ψ and the effective gravitational constant $\tilde{G}_{\rm eff}$. We also consider in the Appendix quasilinear signatures of MG and show how the MG functions affect second order corrections to the power spectrum and the bispectrum.

We discuss in detail what is actually measured by various large-scale structure observations once the assumptions of smooth dark energy and GR are dropped. While lensing and dynamical probes have a direct connection to different potential variables, tracers of the density field and cluster abundances must be treated carefully in extracting information about the density field from them. The most robust tests of MG effects can be made by combining different observables from planned multicolor imaging

surveys and redshift surveys: see Sec. III B for two examples that will be feasible in the near future.

Observables that may not be useful in constraining smooth DE can be crucial for testing MG because there are more variables to be measured and different observables are sensitive to them. For instance, the redshift space power spectrum $P_{g\theta}$ is not considered a valuable probe of structure formation in DE studies as other methods produce lower statistical errors on dark energy parameters. But in a MG scenario, $P_{g\theta}$ is useful because it probes the Newtonian potential ψ that other probes are not sensitive to. It can be combined with galaxy–galaxy lensing, which probes $P_{g(\psi+\phi)}$, to constrain the ratio of potentials ϕ/ψ (Sec. III B). This is a case where observables from multicolor imaging surveys and spectroscopic surveys must be combined to test MG theories. More generally, once one allows for MG scenarios, multiple observables are needed to test theories. Thus the diversity of LSS observations, which has lost some of its appeal in the recent trend of going after a single dark energy figure of merit, becomes vital (see [81] for a broader criticism of dark energy driven research, and [82] for a rebuttal).

Finally we consider a question posed recently in the literature: can a DE model be constructed to mimic any MG theory? We show that with observations of multiple perturbed variables (three are sufficient in general), unique signatures of MG theories can be established. We show with the example of the flat DGP model how, given sufficiently accurate measurements of the lensing and Newtonian potentials and the density, no DE model can mimic the DGP model.

Our results may be compared with other recent studies in the literature, some of which appeared while this work was in progress [19,24,83]. These studies tackle the question of how dark energy and modified gravity can be distinguished. We have clarified the apparent conflicts between this paper and [19] in Sec. IV B. References [24,83,84] present a formal argument that any deviation from GR can be absorbed into the dark sector as an effective dark component. The effective stress-energy tensor of this component, $T^{\rm eff}_{\mu\nu}$, is defined as the deviation of the given MG theory from Einstein's field equations. $T^{\rm eff}_{\mu\nu}$ is conserved, as expected for the usual DE model. From this argument, one might conclude that MG cannot be distinguished from DE gravitationally. However, Hu and Sawicki and Bashinsky [24,83] also pointed out that the effective dark component has a generic, though implicit, coupling to matter, despite the conservation of $T^{\rm eff}_{\mu\nu}$. This coupling hides in the closure relations for this dark component, which depend on external matter and the metric, instead of just its internal microphysics. A theory with such a dark component is different from conventional DE models of the kind we have considered, even ones with strong clustering of the DE. (Indeed, it should not be surprising that allowing for a dark component with an arbitrary stress-energy tensor *and* couplings to matter can mimic any modification of gravity.) Our result, that DE models—with no coupling to matter—can be distinguished from MG, appears to be consistent with the analysis of [24,83]. In Sec. IV we showed how consistency relations, obtained from the evolution and constraint equations obeyed by perturbation variables, help to distinguish between DE and MG. The violation of the consistency conditions that can occur with sufficient observables (see Sec. IV B) would thus imply either the modification of gravity or a coupling of the ''dark energy'' with matter in a GR scenario.

There are several assumptions and caveats in this study. We study MG theories with scalar perturbations to the metric; our formalism does not apply to theories with additional vector or tensor degrees of freedom. While describing the quasilinear regime of large-scale structure (where planned observations have the best signal-to-noise ratio), one needs to be aware that it is not clear how to obtain nonlinear predictions of some MG theories. We have chosen to work in Fourier space, where the description of clustering is simpler, but this means that there is not always a direct relationship of our effective functions for MG theories with the real space description of these theories (e.g., $\tilde{G}_{\rm eff}$ is related to its real space counterpart in the Poisson equation by a convolution with the density field). And finally, we have left for future work a detailed study of the accuracy with which MG tests can be performed by the next generation of surveys.

ACKNOWLEDGMENTS

We are grateful to Jacek Guzik, Eric Linder, and Wayne Hu for helpful discussions and comments on an early draft. We thank Francis Bernardeau, Raul Jimenez, Matt Martino, Roman Scoccimarro, Ravi Sheth, Fritz Stabenau, Masahiro Takada, Jean-Philippe Uzan, and Licia Verde for stimulating discussions. PJ. Z. is supported by the one-hundred talents program of the Chinese Academy of Science (CAS), the National Science Foundation of China Grant No. 10533030, and CAS Grant No. KJCX3-SYW-N2. B. J. is supported in part by NSF Grant No. AST-0607667, the Department of Energy, and the Research Corporation.

APPENDIX: PERTURBATION THEORY IN MODIFIED GRAVITY

The fluid equations in the Newtonian regime are given by the continuity, Euler, and Poisson equations. Keeping the nonlinear terms that have been discarded in the study of linear perturbations in the rest of the paper, the continuity equation gives

$$\dot{\delta} + \theta = -\int \frac{d^3k_1}{(2\pi)^3} \frac{\vec{k}\cdot\vec{k}_1}{k_1^2}\theta(\vec{k}_1)\delta(\vec{k}-\vec{k}_1), \qquad \text{(A1)}$$

where the term on the right shows the nonlinear coupling of

modes. Note that the time derivatives are with respect to conformal time in this Appendix. The Euler equation is

$$\dot{\theta} + H\theta - k^2\psi = -\int \frac{d^3k_1}{(2\pi)^3} \frac{k^2 \vec{k}_1 \cdot (\vec{k} - \vec{k}_1)}{2k_1^2 |\vec{k}_1 - \vec{k}_2^2|^2} \times \theta(\vec{k}_1)\theta(\vec{k} - \vec{k}_1). \quad \text{(A2)}$$

We neglect pressure and anisotropic stress as the energy density is taken to be dominated by nonrelativistic matter [85]. The Poisson equation is given by Eq. (12) and supplemented by the relation between ψ and ϕ given by Eq. (13). Using these equations we can substitute for ψ in the Euler equation to get

$$\dot{\theta} + H\theta + \frac{8\pi\tilde{G}_{\rm eff}}{(1+\eta)}\bar{\rho}_{\rm MG}a^2\delta = -\int \frac{d^3k_1}{(2\pi)^3} \frac{k^2 \vec{k}_1 \cdot (\vec{k} - \vec{k}_1)}{2k_1^2 |\vec{k}_1 - \vec{k}_2^2|^2} \times \theta(\vec{k}_1)\theta(\vec{k} - \vec{k}_1). \quad \text{(A3)}$$

Equations (A1) and (A3) are two equations for the two variables δ and θ. They constitute a fully nonlinear description of MG theories and can be solved once η and $\tilde{G}_{\rm eff}$ are specified. An important caveat is that they may nevertheless be invalid for particular theories, for example, if the superposition principle is violated.

Next we consider perturbative expansions for the density field and the resulting behavior of the power spectrum and bispectrum. Let $\delta = \delta_1 + \delta_2 + \ldots$, where $\delta_2 \sim O(\delta_1^2)$. Higher order effects due to gravitational dynamics become detectable on 10 s of Mpc at low redshift. While this is strictly true only for general relativity, any MG theory that is close enough to GR to fit observations can also be expected to have this feature. In the quasilinear regime, i.e., on length scales between ~10–100 Mpc, mode-coupling effects can be calculated using perturbation theory. For MG, let us simplify the notation by introducing the function:

$$\zeta_{\rm MG}(k,t) = \frac{8\pi\tilde{G}_{\rm eff}}{(1+\eta)}, \quad \text{(A4)}$$

which is simply $4\pi G$ in GR but can vary with time and scale in MG theories. The evolution of the linear growth factor is given by substituting for ψ in Eq. (A5) to get

$$\ddot{\delta}_1 + H\dot{\delta}_1 - \zeta_{\rm MG}\bar{\rho}_{\rm MG}a^2\delta_1 = 0. \quad \text{(A5)}$$

In GR, the relation of ψ to δ is given by the Poisson equation with constant G. In MG, this relation involves both η and $\tilde{G}_{\rm eff}$. If either of these functions have a dependence on k or z, then the solution for the growth factor changes. The linear solutions for ψ and $\psi + \phi$ are then simply obtained using Eqs. (12) and (13).

We show below that in addition the second order solution has a functional dependence on $\tilde{G}_{\rm eff}$ and η that can differ. Thus potentially distinct signatures of the scale and time dependence of $\tilde{G}_{\rm eff}(k,z)$ can be inferred from higher order terms. These rely either on features in k and t in measurements of $P_{\psi+\phi}$ and P_δ, or on the three-point functions, which even at a single redshift can have distinct signatures of MG [86]. Quasilinear signatures due to $\eta(k,z)$ can also be detected via second order terms in the redshift distortion relations for the power spectrum and bispectrum. Our discussion generalizes that of [6] who examined a Yukawa-like modification of the Newtonian potential. Note that inclusion of higher order terms in the density field in the quasistatic Newtonian equations is consistent even if higher order terms in the field equations of modified gravity theories are neglected: the latter involve potentials which are taken to be very small in the weak field limit, unlike the density.

1. Second order solution

From a perturbative treatment of Eqs. (A1) and (A3) the second order term for the growth of the density field is given by

$$\ddot{\delta}_2 + H\dot{\delta}_2 - \bar{\rho}_{\rm MG}a^2\zeta_{\rm MG}\delta_2 = HI_1[\dot{\delta}_1, \delta_1] + I_2[\dot{\delta}_1, \dot{\delta}_1] + \dot{I}_1[\dot{\delta}_1, \delta_1], \quad \text{(A6)}$$

where I_1 and I_2 denote convolutionlike integrals of the two arguments shown, given by the right-hand side of Eqs. (A1) and (A3) as follows:

$$I_1[\dot{\delta}_1, \delta_1](\vec{k}) = \int \frac{d^3k_1}{(2\pi)^3} \frac{\vec{k} \cdot \vec{k}_1}{k_1^2} \dot{\delta}_1(\vec{k}_1)\delta_1(\vec{k} - \vec{k}_1), \quad \text{(A7)}$$

and

$$I_2[\dot{\delta}_1, \dot{\delta}_1](\vec{k}) = \int \frac{d^3k_1}{(2\pi)^3} \frac{k^2 \vec{k}_1 \cdot (\vec{k} - \vec{k}_1)}{2k_1^2 |\vec{k}_1 - \vec{k}_2^2|^2} \dot{\delta}_1(\vec{k}_1)\dot{\delta}_1(\vec{k} - \vec{k}_1). \quad \text{(A8)}$$

Finally, the last term in Eq. (A6) is simply $\dot{I}_1[\dot{\delta}_1, \delta_1] = I_1[\ddot{\delta}_1, \delta_1] + I_1[\dot{\delta}_1, \dot{\delta}_1]$. Note that by continuing the iteration higher order solutions can be obtained.

From the above equations it follows that if $\zeta_{\rm MG} \equiv \zeta_{\rm MG}(t)$ then δ_2 may be specified by k integrals over δ_1, so that one may express the functional relationship $\delta_2 \equiv \delta_2[\delta_1]$ (where it is understood that δ_2 at a given wave number $\vec{k}$ depends on δ_1 at all other wave numbers). But for the general case of a MG theory with scale dependent $\zeta_{\rm MG}$, the second order solution has additional scale and time dependence behavior that is not determined by the linear solution [owing to the third term on the left-hand side in Eq. (A6)]. So the functional relationship must be modified to $\delta_2 \equiv \delta_2[\delta_1; \zeta_{\rm MG}]$. This means that quasilinear evolution provides an additional signature of MG. That is, even if the initial power spectrum is not fully specified (e.g., if the running of the spectral index is not well constrained), the comparison of linear and quasilinear growth rates can reveal the signature of MG. In practice, whether the quasilinear signature is significant must be determined

by computations for specific models (see [87] for a specific model for which it is not). Note also that the second order correction to the density power spectrum also involves the third order density field as it is given by $P_2 \sim \langle\delta_2^2\rangle + \langle\delta_1\delta_3\rangle$. The qualitative features we highlight for δ_2 will also be found in δ_3, which is also given by iterations of the nonlinear Eqs. (A1) and (A2).

We summarize the comparison of linear and second order solutions for the density for GR versus MG. We have identified the function $\zeta_{\rm MG}(k, t)$ as containing all the information about MG that affects density and velocity fields. For the density field the first and second order solutions can be compared to GR as follows:

(i) *Linear growth in GR*: In smooth dark energy GR models, $\delta_1(\vec{k}, t)$ is a separable function of scale and time.

(ii) *Linear growth in MG*: In MG theories, $\delta_1(\vec{k}, t)$ is a separable function of k and t if and only if the MG function $\zeta_{\rm MG}$ is independent of scale.

(iii) *Second order solution in GR*: In smooth dark energy GR models, the second order solution $\delta_2(\vec{k}, t)$ is not separable. It is however determined by integrals over δ_1.

(iv) *Second order solution in MG*: In MG models with $\zeta_{\rm MG}(k, t)$, δ_2 is no longer determined solely by δ_1 and contains additional signatures of MG.

Note that for weak lensing measurements, quasilinear corrections are given by the density times $\tilde{G}_{\rm eff}$ [by substituting higher order terms into Eq. (19)]. So the resulting signatures can be straightforwardly computed using the higher order solutions for the density field.

2. Three-point correlations

Distinct quasilinear effects are found in three-point correlations (we will use the Fourier space bispectrum), as it is the lowest order probe of gravitationally induced non-Gaussianity. The bispectrum for the density field B_δ is defined by

$$\langle\delta(\vec{k}_1)\delta(\vec{k}_2)\delta(\vec{k}_3)\rangle = (2\pi)^3\delta_{\rm D}(\vec{k}_1 + \vec{k}_2 + \vec{k}_3)B_\delta(\vec{k}_1, \vec{k}_2, \vec{k}_3). \tag{A9}$$

Since $B_\delta \sim \langle\delta^3\rangle \sim \langle\delta_1^2\delta_2\rangle$ (using $\langle\delta_1^3\rangle = 0$ for an initially Gaussian density field), the second order solution enters at leading order in the bispectrum. Note also that the wave vector arguments of the bispectrum form a triangle due to the Dirac delta function on the right-hand side above. In practice, a very useful measure of non-Gaussianity is the reduced bispectrum function Q, which for the density field δ is given by

$$Q_\delta \equiv \frac{B_\delta(\vec{k}_1, \vec{k}_2, \vec{k}_3)}{P_\delta(k_1)P_\delta(k_2) + P_\delta(k_2)P_\delta(k_3) + P_\delta(k_1)P_\delta(k_3)}. \tag{A10}$$

To leading order Q is independent of the amplitude of the linear power spectrum [both numerator and denominator are $O(\delta_1^4)$, see [86]] and is nearly constant with triangle size in GR. It is however sensitive to the shape of the triangle. The dependence on size and shape changes for MG theories and is in principle a probe of $\zeta_{\rm MG}$. It is beyond the scope of this paper to elaborate on the measurement of the bispectrum from galaxy surveys; we will instead focus on the prospects for lensing measurements. Shirata *et al.* [71] have tested Yukawa-like modifications of gravity using Q for the galaxy density measured in real and redshift space.

The lensing bispectrum contains perhaps the clearest signature of MG. It is a projection of the three-dimensional bispectrum

$$\begin{aligned} k^6 B_{\psi+\phi} &\sim (8\pi\tilde{G}_{\rm eff}a^2\bar{\rho}_{\rm MG})^3\langle\delta^3\rangle \\ &\simeq (8\pi\tilde{G}_{\rm eff}a^2\bar{\rho}_{\rm MG})^3\langle\delta_1^2\delta_2\rangle. \end{aligned} \tag{A11}$$

Since both δ_1 and δ_2 are functions of $\zeta_{\rm MG}$, measurements of $B_{\psi+\phi}$ are sensitive to $\tilde{G}_{\rm eff}$ and $\zeta_{\rm MG}$ separately.

The reduced lensing bispectrum in a MG theory can be expressed in terms of the density power spectrum and bispectrum as

$$Q_{\psi+\phi} \propto \frac{\tilde{G}_{\rm eff}(k_1)\tilde{G}_{\rm eff}(k_2)\tilde{G}_{\rm eff}(k_3)B_\delta(\vec{k}_1, \vec{k}_2, \vec{k}_3)/\bar{\rho}_{\rm MG}}{k_3^2\tilde{G}_{\rm eff}^2(k_1)P_\delta(k_1)\tilde{G}_{\rm eff}^2(k_2)P_\delta(k_2)/k_1^2k_2^2 + \text{sym}\ldots}. \tag{A12}$$

For equilateral triangles, Q in MG theories is simpler since the $G_{\rm eff}$ factors in all the terms are the same. One then has

$$Q_{\psi+\phi({\rm MG})} \propto \frac{k^2 Q_{\delta({\rm MG})}}{\tilde{G}_{\rm eff}\bar{\rho}_{\rm MG}}. \tag{A13}$$

The ratio of Q for MG versus GR for equilateral triangles is given by

$$\frac{Q_{\psi+\phi({\rm MG})}}{Q_{\psi+\phi({\rm GR})}} \propto \frac{Q_{\delta({\rm MG})}}{Q_{\delta({\rm GR})}}\frac{G\bar{\rho}_{\rm GR}}{\tilde{G}_{\rm eff}\bar{\rho}_{\rm MG}}. \tag{A14}$$

Note that Q_δ itself depends on $\zeta_{\rm MG}$. Bernardeau [86] shows that with $\eta = 1$ but a scale dependent $\tilde{G}_{\rm eff}$, Q_δ for given initial power spectrum is relatively insensitive to $\zeta_{\rm MG}$. If that holds for generic initial power spectra and gravity models, it would imply that $Q_{\psi+\phi({\rm MG})}$ probes $\tilde{G}_{\rm eff}$ for models with $\eta = 1$.

In general a measurement of the lensing power spectrum and reduced bispectrum (roughly speaking, of $P_{\psi+\phi}$ and $Q_{\psi+\phi}$) is sufficient to measure departures from GR. There are three underlying functions (P_δ, $\zeta_{\rm MG}$, and $\tilde{G}_{\rm eff}$) to be determined. For given k and source redshift, we have measurements of P and of Q as a function of triangle shape. Thus while the equilateral triangles may be regarded as sensitive primarily to $\tilde{G}_{\rm eff}$, elongated triangles will be sensitive to $\zeta_{\rm MG}$, and therefore to η. In practice one must take into account the fact that the bispectrum has lower signal-to-noise ratio than the power spectrum on quasi-

linear scales [88], so one must fit for the desired information from all triangle configurations and sizes to constrain the MG functions.

To summarize this section, quasilinear effects thus offer two signatures of MG.

(i) A scale and time dependent feature on quasilinear scales in the power spectrum that depends on η and $\tilde{G}_{\rm eff}$. This enters through the second order contribution to the power spectrum.

(ii) Signatures in the bispectrum: additional signatures of modified gravity are present in three-point correlations of the density and potential fields. Independent of the shape and amplitude of the power spectrum, the dependence of the reduced bispectrum Q on triangle size and shape is a useful test of MG. The reduced lensing bispectrum, for example, has a strong dependence on $\tilde{G}_{\rm eff}$.

We have not considered here whether a clustered DE model can mimic both these signatures. It would be of interest to carry out the second order calculations for a set of MG models and compare predicted deviations with observational error bars.

[1] See, e.g., D. Spergel *et al.*, Astrophys. J. Suppl. Ser. **170**, 377 (2007); M. Tegmark *et al.*, Phys. Rev. D **74**, 123507 (2006); A. Riess *et al.*, Astrophys. J. **659**, 98 (2007).

[2] M. Milgrom, Astrophys. J. **270**, 371 (1983); Jacob D. Bekenstein, Phys. Rev. D **70**, 083509 (2004).

[3] G. Dvali, G. Gabadadze, and M. Porrati, Phys. Lett. B **485**, 208 (2000); C. Deffayet, Phys. Lett. B **502**, 199 (2001).

[4] S. M. Carroll, V. Duvvuri, M. Trodden, and M. S. Turner, Phys. Rev. D **70**, 043528 (2004); S. M. Carroll, A. De Felice, V. Duvvuri, D. A. Easson, M. Trodden, and M. S. Turner, Phys. Rev. D **71**, 063513 (2005).

[5] V. Sahni, Y. Shtanov, and A. Viznyuk, J. Cosmol. Astropart. Phys. 12 (2005) 5.

[6] M. White and C. S. Kochanek, Astrophys. J. **560**, 539 (2001); A. Shirata, T. Shiromizu, N. Yoshida, and Y. Suto, Phys. Rev. D **71**, 064030 (2005); C. Sealfon, L. Verde, and R. Jimenez, Phys. Rev. D **71**, 083004 (2005); H. Stabenau and B. Jain, Phys. Rev. D **74**, 084007 (2006); M. Sereno and J. A. Peacock, Mon. Not. R. Astron. Soc. **371**, 719 (2006); A. Shirata, Y. Suto, C. Hikage, T. Shiromizu, and N. Yoshida, Phys. Rev. D **76**, 044026 (2007).

[7] C. Skordis, D. F. Mota, P. G. Ferreira, and C. Boehm, Phys. Rev. Lett. **96**, 011301 (2006); C. Skordis, Phys. Rev. D **74**, 103513 (2006).

[8] S. Dodelson and M. Liguori, Phys. Rev. Lett. **97**, 231301 (2006).

[9] A. Lue, R. Scoccimarro, and G. Starkman, Phys. Rev. D **69**, 124015 (2004).

[10] L. Knox, Y.-S. Song, and J. A. Tyson, arXiv:astro-ph/0503644; M. Ishak, A. Upadhye, and D. N. Spergel, Phys. Rev. D **74**, 043513 (2006).

[11] K. Koyama and R. Maartens, J. Cosmol. Astropart. Phys. 01 (2006) 016.

[12] T. Koivisto and H. Kurki-Suonio, Classical Quantum Gravity **23**, 2355 (2006); T. Koivisto, Phys. Rev. D **73**, 083517 (2006); B. Li and M.-C. Chu, Phys. Rev. D **74**, 104010 (2006); Y.-S. Song, W. Hu, and I. Sawicki, Phys. Rev. D **75**, 044004 (2007); B. Li and J. Barrow, Phys. Rev. D **75**, 084010 (2007); M. Amarzguioui, Ø. Elgarøy, D. F. Mota, and T. Multamäki, Astron. Astrophys. **454**, 707 (2006).

[13] P. Zhang, Phys. Rev. D **73**, 123504 (2006).

[14] R. Bean, D. Bernat, L. Pogosian, A. Silvestri, and M. Trodden, Phys. Rev. D **75**, 064020 (2007).

[15] E. Linder, Phys. Rev. D **72**, 043529 (2005); D. Huterer and E. Linder, Phys. Rev. D **75**, 023519 (2007).

[16] J.-P. Uzan, Gen. Relativ. Gravit. **39**, 307 (2007).

[17] R. Caldwell, C. Cooray, and A. Melchiorri, Phys. Rev. D **76**, 023507 (2007).

[18] L. Amendola, M. Kunz, and D. Sapone, J. Cosmol. Astropart. Phys. 04 (2008) 013.

[19] M. Kunz and D. Sapone, Phys. Rev. Lett. **98**, 121301 (2007).

[20] C.-P. Ma and E. Bertschinger, Astrophys. J. **455**, 7 (1995).

[21] W. Hu and D. J. Eisenstein, Phys. Rev. D **59**, 083509 (1999).

[22] M. Kunz, arXiv:astro-ph/0702615.

[23] E. Bertschinger, Astrophys. J. **648**, 797 (2006).

[24] W. Hu and I. Sawicki, Phys. Rev. D **76**, 104043 (2007).

[25] P. Zhang, M. Liguori, R. Bean, and S. Dodelson, Phys. Rev. Lett. **99**, 141302 (2007).

[26] We thank Eric Linder for pointing out the caveat about real and Fourier space treatments.

[27] B. Boisseau, G. Esposito-Farèse, D. Polarski, and A. A. Starobinsky, Phys. Rev. Lett. **85**, 2236 (2000).

[28] C. M. Will, Living Rev. Relativity **9**, 3 (2006).

[29] A. S. Bolton, S. Rappaport, and S. Burles, Phys. Rev. D **74**, 061501 (2006).

[30] Cedric Deffayet and Kristen Menou, arXiv:0709.0003.

[31] S. Carroll, *Spacetime and Geometry* (Addison-Wesley, Reading, MA, 2004).

[32] W. Hu, Astrophys. J. **522**, L21 (1999).

[33] R. Caldwell, A. Cooray, and A. Melchiorri, Phys. Rev. D **76**, 023507 (2007).

[34] J. P. Uzan and F. Bernardeau, Phys. Rev. D **64**, 083004 (2001).

[35] A. F. Heavens, T. D. Kitching, and L. Verde, Mon. Not. R. Astron. Soc. **380**, 1029 (2007).

[36] V. Acquaviva and L. Verde, J. Cosmol. Astropart. Phys. 12 (2007) 001.

[37] M. A. Amin, R. V. Wagoner, and R. D. Blandford, arXiv:0708.1793.

[38] S. Tsujikawa, Phys. Rev. D **76**, 023514 (2007).

[39] D. Clowe, M. Bradač, A. H. Gonzalez, M. Markevitch, S. W. Randall, C. Jones, and D. Zaritsky, Astrophys. J.

648, L109 (2006).
[40] W. Hu and B. Jain, Phys. Rev. D **70**, 043009 (2004).
[41] U. Seljak, A. Slosar, and P. McDonald, J. Cosmol. Astropart. Phys. 10 (2006) 14.
[42] A. Klypin and F. Prada, arXiv:0706.3554.
[43] R. Scoccimarro, Phys. Rev. D **70**, 083007 (2004).
[44] M. Tegmark, A. Hamilton, and Y. Xu., Mon. Not. R. Astron. Soc. **335**, 887 (2002).
[45] M. Tegmark *et al.*, Astrophys. J. **606**, 702 (2004).
[46] See, e.g., Y. P. Jing, H. J. Mo, and G. Boerner, Astrophys. J. **494**, 1 (1998); Y. P. Jing, Gerhard Boerner, and Yasushi Suto, Astrophys. J. **564**, 15 (2002); Y. P. Jing and G. Boerner, Astrophys. J. **617**, 782 (2004).
[47] P. J. Zhang *et al.* (unpublished).
[48] See J. L. Tinker, Mon. Not. R. Astron. Soc. **374**, 477 (2007), for efforts to improve the redshift distortion in real space.
[49] F. Bernardeau, S. Colombi, E. Gaztañaga, and R. Scoccimarro, Phys. Rep. **367**, 1 (2002).
[50] A. J. Connolly *et al.*, Astrophys. J. **579**, 42 (2002); S. Dodelson *et al.*, Astrophys. J. **572**, 140 (2002); M. Tegmark *et al.*, Astrophys. J. **571**, 191 (2002); A. S. Szalay *et al.*, Astrophys. J. **591**, 1 (2003).
[51] H. J. Mo and S. D. M. White, Mon. Not. R. Astron. Soc. **282**, 347 (1996).
[52] A. Cooray and R. Sheth, Phys. Rep. **372**, 1 (2002).
[53] J. A. Frieman and E. Gaztanaga, Astrophys. J. **425**, 392 (1994).
[54] J. N. Fry, Phys. Rev. Lett. **73**, 215 (1994).
[55] E. Pierpaoli, S. Borgani, D. Scott, and M. White, Mon. Not. R. Astron. Soc. **342**, 163 (2003).
[56] See, e.g., L. R. Abramo, R. C. Batista, L. Liberato, and R. Rosenfeld, J. Cosmol. Astropart. Phys. 11 (2007) 012.
[57] See, e.g., M. J. Hudson, R. J. Smith, J. Lucey, and E. Branchini, Mon. Not. R. Astron. Soc. **352**, 61 (2004); H. Feldman *et al.*, Astrophys. J. **596**, L131 (2003); D. Sarkar, H. A. Feldman, and R. Watkins, Mon. Not. R. Astron. Soc. **375**, 691 (2007), and references therein.
[58] For recent measurements, see, e.g., C. Bonvin, R. Durrer, and M. Kunz, Phys. Rev. Lett. **96**, 191302 (2006); T. Haugboelle, S. Hannestad, B. Thomsen, J. Fynbo, J. Sollerman, and S. Jha, Astrophys. J. **661**, 650 (2007); L. F. Wang, arXiv:0705.0368 [Ap. J. (to be published)]; R. Watkins and H. A. Feldman, Mon. Not. R. Astron. Soc. **379**, 343 (2007).
[59] R. Sunyaev and Y. Zel'dovich, Mon. Not. R. Astron. Soc. **190**, 413 (1980).
[60] M. G. Haehnelt and M. Tegmark, Mon. Not. R. Astron. Soc. **279**, 545 (1996); A. Kashlinsky and Atrio–Barandela, Astrophys. J. **536**, L67 (2000); N. Aghanim, K. M. Gorski, and J. L. Puget, Astron. Astrophys. **374**, 1 (2001); F. Atrio-Barandela, A. Kashlinsky, and J. P. Mucket, Astrophys. J. **601**, L111 (2004); G. Holder, Astrophys. J. **602**, 18 (2004); P. Zhang, H. Feldman, R. Juszkiewicz, and A. Stebbins, Mon. Not. R. Astron. Soc. **388**, 884 (2008).
[61] R. K. Sachs and A. M. Wolfe, Astrophys. J. **147**, 73 (1967).
[62] See, e.g., A. Cabre, E. Gaztanaga, M. Manera, P. Fosalba, and F. Castander, Mon. Not. R. Astron. Soc. **372**, L23 (2006); Davide Pietrobon, Amedeo Balbi, and Domenico Marinucci, Phys. Rev. D **74**, 043524 (2006); Tommaso Giannantonio *et al.*, Phys. Rev. D **74**, 063520 (2006), and references therein.
[63] U. Seljak and M. Zaldarriaga, Phys. Rev. D **60**, 043504 (1999).
[64] P. J. Zhang, Astrophys. J. **647**, 55 (2006).
[65] P. Fosalba and O. Dor., Phys. Rev. D **76**, 103523 (2007).
[66] U. Seljak and M. Zaldarriaga, Phys. Rev. Lett. **82**, 2636 (1999); M. Zaldarriaga and U. Seljak, Phys. Rev. D **59**, 123507 (1999); W. Hu and T. Okamoto, Astrophys. J. **574**, 566 (2002); Oliver Zahn and Matias Zaldarriaga, Astrophys. J. **653**, 922 (2006).
[67] Both DE and MG models exist with observational consequences at redshifts significantly higher than 1: these include oscillating w models and TeVeS (see also [24,36]). Future surveys will provide some probes of this higher redshift universe through effects such as CMB lensing, high-z galaxy surveys and 21 cm redshift space measurements.
[68] http://www.skatelescope.org/.
[69] F. B. Abdalla and S. Rawlings, Mon. Not. R. Astron. Soc. **360**, 27 (2005).
[70] P. Zhang and U.-L. Pen, Phys. Rev. Lett. **95**, 241302 (2005); Mon. Not. R. Astron. Soc. **367**, 169 (2006).
[71] A. Shirata, Y. Suto, C. Hikage, T. Shiromizu, and N. Yoshida, Phys. Rev. D **76**, 044026 (2007).
[72] E. Sheldon *et al.*, Astrophys. J. **127**, 2544 (2004).
[73] R. Mandelbaum, U. Seljak, G. Kauffmann, C. M. Hirata, and J. Brinkmann, Mon. Not. R. Astron. Soc. **368**, 715 (2006).
[74] J. Zhang, L. Hui, and A. Stebbins, Astrophys. J. **635**, 806 (2005).
[75] T. Chiba and R. Takahashi, Phys. Rev. D **75**, 101301 (2007).
[76] S. Wang, L. Hui, M. May, and Z. Haiman, Phys. Rev. D **76**, 063503 (2007).
[77] R. Bean and O. Dor., Phys. Rev. D **69**, 083503 (2004); J. Weller and A. M. Lewis, Mon. Not. R. Astron. Soc. **346**, 987 (2003); Jun-Qing Xia, Yi-Fu Cai, Tao-Tao Qiu, Gong-Bo Zhao, and Xinmin Zhang, arXiv:astro-ph/0703202.
[78] T. Koivisto and D. F. Mota, Phys. Rev. D **73**, 083502 (2006); D. F. Mota, J. R. Kristiansen, T. Koivisto, and N. E. Groeneboom, arXiv:0708.0830.
[79] Notice that this DE model has large dark energy fluctuations on scales well below the horizon, so it differs from conventional clustered DE models that rely on scalar field dynamics. Furthermore, usually δp is parametrized as $\delta p = c_s^2 \delta\rho$ (c_s can be both scale and time dependent). The DE model considered by [19] has an unusual form of pressure perturbation, in which δp is connected to the anisotropic stress σ instead of δ.
[80] W. Hu, Astrophys. J. **506**, 485 (1998).
[81] S. D. M. White, Rep. Prog. Phys. **70**, 883 (2007).
[82] R. Kolb, Rep. Prog. Phys. **70**, 1583 (2007).
[83] S. Bashinsky, arXiv:0707.0692.
[84] L. Pogosian and A. Silvestri, Phys. Rev. D **77**, 023503 (2008).
[85] B. Jain and E. Bertschinger, Astrophys. J. **431**, 495 (1994).
[86] F. Bernardeau, arXiv:astro-ph/0409224.
[87] H. Stabenau and B. Jain, Phys. Rev. D **74**, 084007 (2006).
[88] M. Takada and B. Jain, Mon. Not. R. Astron. Soc. **348**, 897 (2004).